https://doi.org/10.5194/acp-2019-966
Preprint. Discussion started: 17 January 2020

Atmospheric Chemistry and Physics Discussions

The haze pollution under strong atmospheric oxidization capacity in summer in Beijing: Insights into the formation mechanism of atmospheric physicochemical process

Dandan Zhao[†1,2]; Guangjing Liu[†3,1]; Jinyuan Xin[*1,2,4]; Jiannong Quan[5]; Yuesi Wang[1]; Xin Wang[3]; Lindong Dai[1]; Wenkang Gao[1]; Guiqian Tang[1]; Bo Hu[1]; Yongxiang Ma[1]; Xiaoyan Wu[1]; Lili Wang[1]; Zirui Liu[1]; Fangkun Wu[1]

1 State Key Laboratory of Atmospheric Boundary Layer Physics and Atmospheric Chemistry (LAPC), Institute of Atmospheric Physics, Chinese Academy of Sciences, Beijing 100029, China

2 University of Chinese Academy of Sciences, Beijing 100049, China

3 College of Atmospheric Sciences, Lanzhou University, Lanzhou 730000, China.

4 Collaborative Innovation Center on Forecast and Evaluation of Meteorological Disasters, Nanjing University of Information Science and Technology, Nanjing 210044

5 Institute of Urban Meteorology, Chinese Meteorological Administration, Beijing, China

(†) These authors contributed equally to this study.

(*) Correspondence: Jinyuan Xin (xjy@mail.iap.ac.cn)

Abstract: Under strong atmospheric oxidization capacity, haze pollution in the summer of Beijing was the result of the synergistic effect of physicochemical process in the atmospheric boundary layer (ABL). The south/southwest areas generally ~60-300 km far away from Beijing were seriously polluted, in contrast to a clean situation in Beijing. The southerly winds moving more than ~20-30 km h^{-1} since early morning primarily caused the initiation of haze pollution. The $PM_{2.5}$ level increased to 75 μg m^{-3} in several hours at daytime, which was simultaneously affected by the ABL structure. Additionally, the O_3 concentration was quite high at daytime (250 μg m^{-3}), corresponding to a strong atmospheric oxidation capacity. Numerous sulfate and nitrate were formed through active atmospheric chemical processes, with sulfur oxidation ratio (SOR) up to ~0.76 and nitrogen oxidation ratio (NOR) increasing from 0.09 to 0.26, which further facilitated the particulate matter (PM) level rising. Even so, the increase in sulfate was mainly linked by southerly transport. At midnight, the $PM_{2.5}$ concentration sharply increased from 75 μg m^{-3} to 150 μg m^{-3} in 4 hours and stayed the highest level till the

https://doi.org/10.5194/acp-2019-966
Preprint. Discussion started: 17 January 2020


Atmospheric Chemistry and Physics Discussions

next morning. With the premise of an extremely stable ABL structure, the formation of secondary aerosols dominated by nitrate was quite intense, driving the outbreak of haze pollution. PM levels in the south/southeast of Beijing were significantly lower than that in Beijing over this time, even below air quality standards, thus, the contribution of pollution transport was almost gone. With the formation of nocturnal stable boundary layer of 0-0.3 km altitude, the extremely low turbulence kinetic energy (TKE) of 0-0.05 m^2 s^{-2} inhibited the spread of particles and moisture, ending up with elevated levels of $PM_{2.5}$ and relative humidity (~90 %) near the surface. Under quite high humidity and strong ambient oxidization capacity, the NOR rapidly increased from 0.26 to 0.60 and heterogeneous hydrolysis reactions at the moist particle surface were very significant. The nitrate concentration explosively increased from 11.6 μg m^{-3} to 57.8 μg m^{-3}, while the concentrations of sulfate and organics slightly increased by 6.1 μg m^{-3} and 3.1 μg m^{-3}, respectively. With clean & strong winds passing through Beijing, the stable ABL was broken with potential temperature gradient turning to negative and ABL heights increasing to ~2.5 km. The strong turbulence activity with TKE of ~3-5 m^2 s^{-2} notably promoted the pollution diffusion. The self-cleaning capacity of the atmosphere is always responsible for the dispersion of air pollution. Even so, reducing atmospheric oxidization capacity such as strengthening the collaborative control of nitrogen oxide (NOx) and volatile organic compounds (VOCs) was urgent, as well as continuously deepening regional joint control of air pollution.

1 Introduction

Due to a series of stringent emission control measures (China's State Council 2013 Action Plan for Air Pollution Prevention and Control available at http://gov.cn/zwgk/2013-09/12/), including shutting down heavily polluting factories and replacing coal fuels with clean energies, the annual mean $PM_{2.5}$ (particulate matter with dynamic equivalent diameter less than 2.5 μm) concentration in major regions, especially in Beijing, has dropped continuously in recent years (Chen et al., 2019; Liu et al., 2019a; Cheng et al., 2019a; Ding et al., 2019). However, the ground-level O_3 concentration across China increased rapidly in recent years, especially in summer,

https://doi.org/10.5194/acp-2019-966
Preprint. Discussion started: 17 January 2020


Atmospheric Chemistry and Physics Discussions

despite recent reductions in the emissions of SO_2 and nitrogen oxide (NOx) (Chen et al., 2018; Anger et al., 2016; Wang et al., 2018; Wang et al., 2017b). This discrepancy of variation trend between O_3 and $PM_{2.5}$ may be attributed to the inappropriate reduction ratio of NOx and volatile organic compounds (VOCs) in $PM_{2.5}$-control oriented emission reduction measures which mainly focus on NOx reduction (Liu et al., 2013a; Cheng et al., 2019b). Besides, a number of studies have shown that the reduce in ambient particles can influence the surface ozone generation via changing the heterogeneous reaction and decreasing the photodecomposition rate (O_3 and its precursors) through the aerosol-radiation interaction (Liu et al., 2019b; Wang et al., 2019b; He and Carmichael, 1999; Dickerson et al., 1997; Tie et al., 2001; Martin et al., 2003; Tie et al., 2005). Recently, even though the $PM_{2.5}$ level in Beijing is generally low due to stringent emission control measures, several haze pollution episodes with alternate/synchronous high ozone concentration have still occurred in the summer of 2019. Regarding the causes of particulate matter (PM) pollution, numerous previous studies have reported that the stationary synoptic condition, local emissions and regional transport, adverse atmospheric boundary layer (ABL) structure and meteorology conditions as well as the secondary aerosol formation are major factors in the formation of haze pollution (Li et al., 2019; Sun et al., 2012; Wang et al., 2016; Liu et al., 2019c; Huang et al., 2017; Luan et al., 2018; Han et al., 2019). Huang et al. (2017) demonstrated that haze pollution in the Beijing-Tianjin-Hebei usually occurred when air masses originating from polluted industrial regions in the south prevailed and is characterized by high $PM_{2.5}$ loadings with considerable contributions from secondary aerosols. Bi et al. (2017) stated that strong wind and vertical mixing in daytime scavenged the pollution, and the weak wind and stable inversion layer at night favorably accumulated the air pollutants near the surface. Zhong et al. (2018) showed that the positive ABL meteorological feedback on $PM_{2.5}$ mass concentration explains over 70 % of the outbreak of pollution. Zhao et al. (2019) also pointed out that the constant feedback effect between aerosol radiative forcing and the ABL stability continually reduced atmospheric environmental capacity and aggravated air pollution. The

https://doi.org/10.5194/acp-2019-966
Preprint. Discussion started: 17 January 2020


Atmospheric Chemistry and Physics Discussions

dominated components of PM, including sulfate, nitrate, ammonium, and organics, are mostly formed via the homogeneous/heterogeneous reactions of gas phase precursors in the atmosphere (Orrling et al., 2011; Wang et al., 2016) and account for over 50 % of the $PM_{2.5}$ mass (Wang et al., 2013; Liu et al., 2019a; Sun et al., 2015; Yao et al., 2002). Ming et al. (2017) have proved that the contribution of secondary aerosol formation during haze pollution episodes was much higher than before and after the episodes.

Although the causes of heavy $PM_{2.5}$ loading were widely examined, most of these studies referenced to haze pollution in winter and only involved in one or several key factors. In the summer of Beijing, with strong solar radiation, O_3 can be quickly formed via photochemical reactions among precursors, including volatile organic compounds (VOCs) and nitrogen oxides (NOx), which contributes the increase in ambient oxidizing capacity (Wang et al., 2017c; Ainsworth et al., 2012; Hassan et al., 2013; Trainer et al., 2000; Sillman, 1999). Meteorology conditions, including solar radiation, temperature, relative humidity, wind speed and direction, and cloud cover, also play an important role in short-term ozone variations, further affecting the atmospheric oxidization capacity (Lu et al., 2019; Cheng et al., 2019b; Toh et al., 2013; Wang et al., 2017d; Zeng et al., 2018). As ozone pollution is more and more prominent, and the ability of atmospheric oxidation is gradually stronger, the formation mechanism of haze pollution under strong atmospheric oxidization capacity need to be concerned. Previous studies have demonstrated that strong atmospheric photochemical reactions in summer enhanced secondary aerosols formation and led to the synchronous occurrence of high concentrations of $PM_{2.5}$ and O_3 on a regional scale (Pathak et al., 2009; Wang et al., 2016; Shi et al., 2015). Nevertheless, the mechanisms of how overall regional transport, ABL structure, meteorological conditions and the formation of secondary aerosols work together to quantitatively influence the haze pollution under strong atmospheric oxidization capacity in summer remain unclear. Therefore, with minutely observation of air temperature and relative & absolute humidity profiles, vertical velocity and horizontal wind vector profiles, atmospheric

https://doi.org/10.5194/acp-2019-966
Preprint. Discussion started: 17 January 2020

Atmospheric Chemistry and Physics Discussions

backscattering coefficient (BSC) profiles and ABL heights (ABLH), as well as mass concentration and composition of $PM_{2.5}$, aerosol optical depth (AOD) and mass concentrations of gas pollutants including O_3, SO_2, and NO_2, this paper would comprehensively explore the formation mechanism of haze pollution under strong ambient oxidization capacity insights into atmospheric physics and chemistry, for proposing selected recommendations for model forecast and cause analysis of complex air pollution in the summer of Beijing.

2 Instruments and data

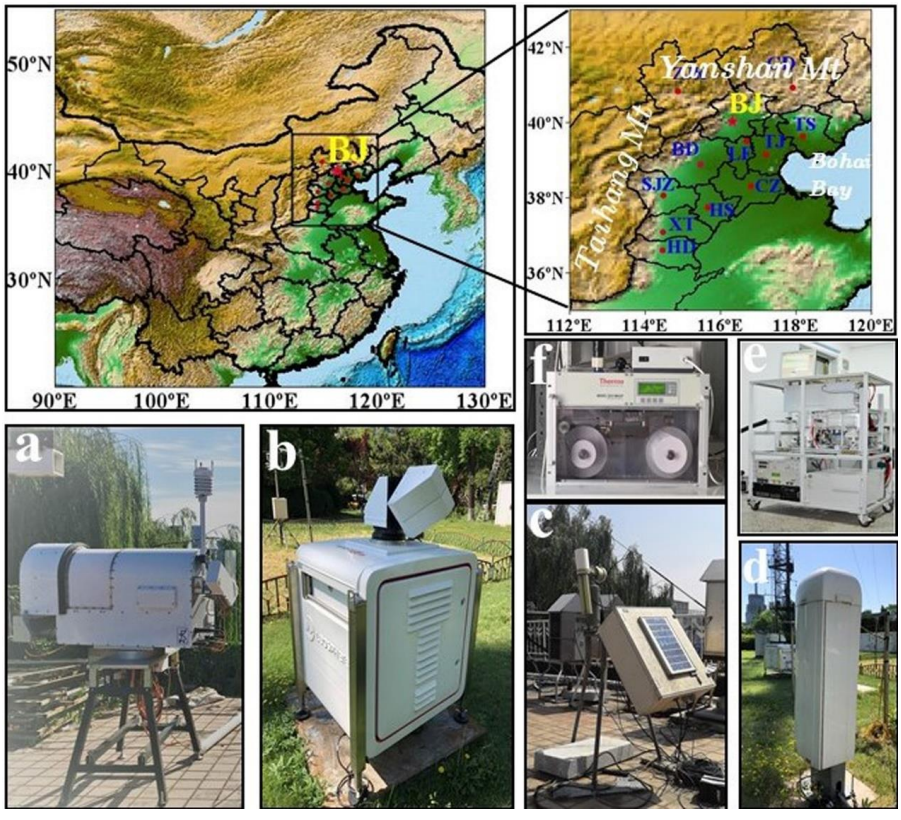

Figure 1. The geographical location of Beijing city (BJ) marked by a red star as well as surrounding regions, and the relevant measurement instruments used in this paper. Left-top panel is the topographic distribution of most of China with Beijing and surrounding areas circled, and right-top panel is the topographic distribution of the Beijing-Tianjin-Hebei (BTH) region, with Yanshan mountains to the north, Taihang Mountains to the west, and Bohai Bay to

https://doi.org/10.5194/acp-2019-966
Preprint. Discussion started: 17 January 2020


Atmospheric Chemistry and Physics Discussions

131 the east. Blue words represent abbreviations for city names in the BTH. The pictures of (a)-(f)
132 are Microwave Radiometer, 3D Doppler Wind Lidar, CIMEL sun-photometer, Ceilometer,
133 Aerodyne Aerosol Chemical Speciation Monitor and Multi-angle Absorption Photometer set in
134 the BJ site.

135 **2.1 Instruments and related data**

136 The observation site was at the Tower Branch of the Institute of Atmospheric
137 Physics, Chinese Academy of Sciences (IAP, 39°58′N, 116°22′E, altitude: 58 m). And
138 the IAP site is located at north ring-3 and north ring-4 of Beijing, China, within
139 educational, commercial and residential areas, a representative for a typical urban site
140 in Beijing (hereinafter BJ site). All the sampling instruments are placed at the same
141 place and operate simultaneous monitoring. All the data used in this paper are from July
142 22 to 27 in 2019 and are reported in Beijing Standard Time.

143 Air temperature and relative & absolute humidity profiles were collected by
144 Microwave Radiometer (RPG-HATPRO-G5 0030109, Germany). The Microwave
145 Radiometer (hereinafter MWR) produces profiles at 10-30 m resolution up to 0.5 km,
146 40-70 m resolution from 0.5 km to 2.5 km and 100-200 m resolution from 2 km to 10
147 km with a temporal resolution of one second. The detailed description of instruments
148 of the RPG-HATPRO type can be found at the Internet site of http://www.radiometer-
149 physics.de.

150 Vertical wind speed and horizontal wind vector profiles were retrieved by 3D
151 scanning Doppler Wind Lidar (Windcube 100s, Leosphere, France). The wind
152 measurement results have a spatial resolution of 1-20 m up to 0.3 km and 25 m from
153 0.3 km to 3 km, with a temporal resolution of one second. More details of this
154 instrument can be looked up at the Internet site of www.leosphere.com.

155 The Ceilometer (CL51, Vaisala, Finland), is responsible for the detection of
156 atmospheric BSC profiles. The CL51 ceilometer digitally samples the return
157 backscattering signal from 0 to 100 μs and provides BSC profiles with a spatial
158 resolution of 10 m from the ground to a height of 15 km. As the PM is almost in the
159 ABL and is barely in the free atmosphere, the ABL height was determined by a sharp

https://doi.org/10.5194/acp-2019-966
Preprint. Discussion started: 17 January 2020


Atmospheric Chemistry and Physics Discussions

change in the negative gradient in the BSC profile (Muenkel et al., 2007). More detailed information on ABL height calculation and screening can be found in previous studies (Tang et al., 2016; Zhu et al., 2018).

Aerosol optical depth (AOD) is observed by the CIMEL sun-photometer (CE318, France) and AOD in 500 nm is used in this paper. CE318 is a multi-channel, automatic sun-and-sky scanning radiometer and takes measurements only during daylight hours (sun above the horizon). Detailed information of the AOD inversion method and the CE318 instrument is introduced in Gregory (2011).

The real-time hourly mean ground-level of $PM_{2.5}$, PM_{10}, O_3, NO_2 and SO_2, were downloaded from the China National Environmental Monitoring Center (CNEMC) (available at http://106.37.208.233:20035/). All operational procedures are conducted strictly following "The Specification of Environmental Air Quality Automatic Monitoring Technology" (HJ/T193-2005, available at http://kjs.mep.gov.cn/hjbhbz/bzwb/dqhjbh/jcgfffbz/200601/t20060101_71675.htm). The chemical species of PM including organics (Org), sulfate (SO_4^{2-}), nitrate (NO_3^-), ammonium (NH_4^+) and chloride (Cl^-) were hourly measured by Aerosol Chemical Speciation Monitor (ACSM). More detailed descriptions for ACSM have been given in Ng et al. (2011). The black carbon (BC) mass concentration is observed by the Multi-angle Absorption Photometer (MAAP5012, Thermo Electron). A more detailed description of this MAAP could be found in Petzold and Schonlinner (2004). As shown in Fig.2, the ACSM $PM_{2.5}$ mass concentration (=organics + sulfate + nitrate + ammonium + chloride + BC) tracked well the online $PM_{2.5}$ mass concentration, which directly observed by the particulate matter analyzer (from the CNEMC), with the correlation coefficient (R^2) of 0.82. On average, the ACSM $PM_{2.5}$ mass concentration reports 80 % of the online $PM_{2.5}$ mass concentration. All chemical compositions measured by the ACSM, including organics, sulfate, nitrate ammonium and chloride, plus the BC can represent the dominant species of $PM_{2.5}$.

https://doi.org/10.5194/acp-2019-966
Preprint. Discussion started: 17 January 2020

Atmospheric Chemistry and Physics Discussions

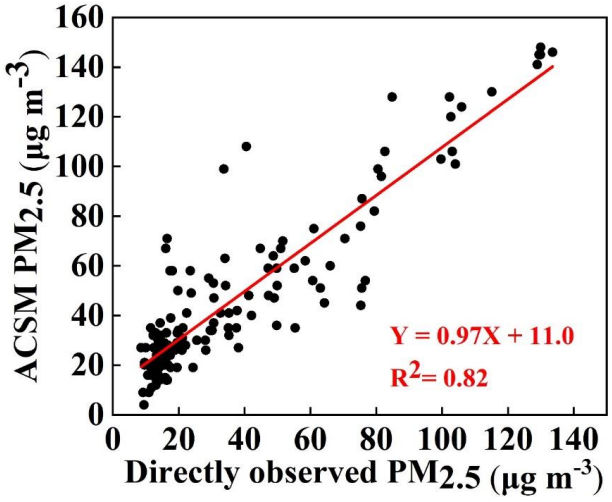

Figure 2. Scatter plot of the relationship between directly observed $PM_{2.5}$ mass concentration by the PM analyzer from the China National Environmental Monitoring Center and calculated $PM_{2.5}$ mass concentration from chemical constituent mass concentration measured by Aerosol Chemical Speciation Monitor plus black carbon mass concentration measured by Multi-angle Absorption Photometer.

2.2 Other datasets

Virtual potential temperature (θ_V) and pseudo-equivalent potential temperature (θ_{se}) are respectively calculated by Eq. (1) and Eq. (2):

$$\theta_v = T(1 + 0.608q)(\frac{1000}{P})^{0.286} \quad (1)$$

$$\theta_{se} = T(\frac{1000}{P})^{0.286} exp\,(\frac{r_s L_v}{C_{pd} T}) \quad (2)$$

where T is air temperature, q is specific humidity, p is air pressure, r_s is saturation mixing ratio, Lv is the latent heat of vaporization of 2.5×10^6 J kg^{-1} and C_{pd} is the specific heat of air of 1005 J kg^{-1} K^{-1}. All the relevant parameters can be calculated from temperature and humidity profile data of MWR, then the values of θ_v and θ_{se} at different altitudes can be obtained further. Hourly turbulence kinetic energy (TKE) is calculated as:

$$TKE = 0.5 \times (\delta_u^2 + \delta_v^2 + \delta_w^2). \quad (3)$$

The one-hour vertical velocity standard deviation (δ_w^2) and the one-hour horizontal wind standard deviation (δ_u^2; δ_v^2) are respectively calculated by Eq. (4) and Eq. (5)-(6):

https://doi.org/10.5194/acp-2019-966
Preprint. Discussion started: 17 January 2020

Atmospheric Chemistry and Physics Discussions

$$\delta_w^2 = \frac{1}{N-1}\sum_{i=1}^{N}(w_i - \bar{w})^2 \quad (4)$$

$$\delta_u^2 = \frac{1}{N-1}\sum_{i=1}^{N}(u_i - \bar{u})^2 \quad (5)$$

$$\delta_v^2 = \frac{1}{N-1}\sum_{i=1}^{N}(v_i - \bar{v})^2 \quad (6)$$

where N is the record number every one hour, w_i denotes the i_{th} vertical wind velocity (m s^{-1}), $u_i(v_i)$ denotes the i_{th} horizontal wind speed (m s^{-1}), $\bar{w}$ is the mean vertical wind speed (m s^{-1}), and $\bar{u}$ ($\bar{v}$) is the mean horizontal wind speed (m s^{-1}) (Wang et al., 2019a; Banta et al., 2006). Atmospheric reanalysis data from the National Centers for Environmental Prediction (NCEP) were collected 4 times daily at 0200, 0800, 1400, and 2000 (LT) with a horizontal resolution of 2.5° × 2.5°.

3 Results and discussion

3.1 Typical air pollution episodes in summer in Beijing

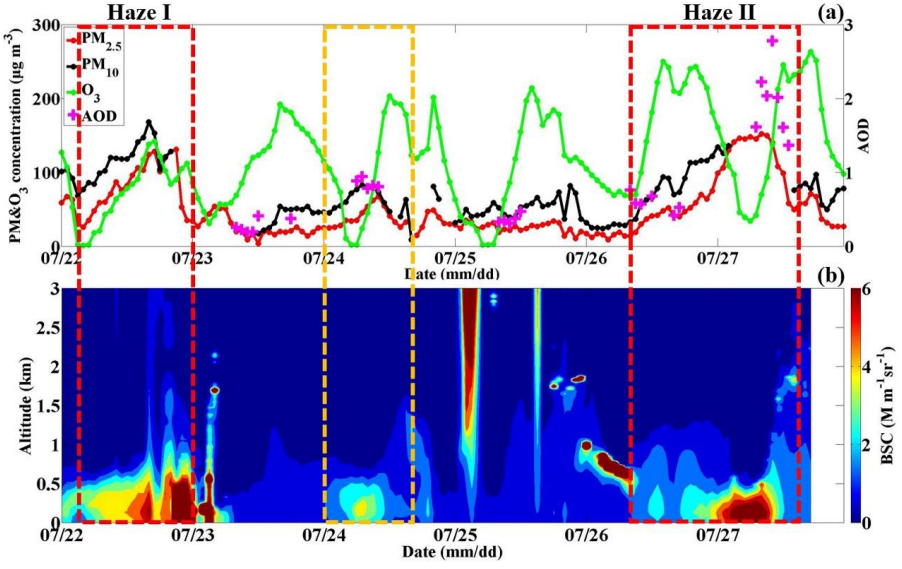

Figure 3. (a) Temporal variation on mass concentrations of $PM_{2.5}$, PM_{10} and O_3 as well as aerosol optical depth (AOD) in the BJ site during July 22-27, 2019; (b) Temporal variation on vertical profiles of atmospheric backscattering coefficient (BSC) in the BJ site during July 22-27, 2019. (The yellow-mark part represents the light haze pollution period and the red-mark part represents heavy haze pollution episode.)

Considering both the daily-mean $PM_{2.5}$ mass concentration on the 22nd and 26th-

https://doi.org/10.5194/acp-2019-966
Preprint. Discussion started: 17 January 2020


Atmospheric Chemistry and Physics Discussions

225 27th exceeded the national secondary standard (75 μg m^{-3}) (GB3095-2012) with
226 maximum hourly average up to 131 μg m^{-3} and 152 μg m^{-3}, respectively, two serious
227 PM pollution processes occurred, defined as Haze I and Haze II, respectively. During
228 the two haze periods, high atmospheric BSC levels mainly distributed below 0.5 km
229 altitude, with values of ~4-6 M m^{-1} sr^{-1}. It reflects the vertical distribution of ambient
230 particles from the aspect of aerosol scattering to some degree, that is, suspended
231 numerous particles just concentrated in the lower atmosphere layer. According to
232 National Ambient Air Quality Standards (GB3095-2012), a day when the hourly-mean
233 O_3 concentration more than 160 μg m^{-3} is regarded as ozone pollution day, thus, there
234 was serious ozone pollution every day during the observation periods. As reported by
235 the Ministry of Ecology and Environment, in 2018, the number of motor vehicles
236 reached 327 million, up 5.5 percent year-on-year (available at
237 http://www.mee.gov.cn/xxgk2018/xxgk/xxgk15/201909/t20190904_732374.html).
238 Although stringent pollution control measures on factories, the number of motor
239 vehicles still discharged a large number of primary pollutants into the atmosphere,
240 including NOx, HC, VOCs, and CO. And with strong solar radiation and high
241 temperature in summer, photochemical processes are prominent, contributing to the
242 high concentration of O_3 along with many highly reactive radicals, which further
243 enhanced the oxidizing capacity of the atmosphere (Frischer et al., 1999; Sharma et al.,
244 2013). Haze pollution under the condition of strong atmospheric oxidation capacity was
245 thought to respectively occur on the 22nd and 26th-27th. Generally, under stringent
246 pollutants emission control measures, the emission of primary aerosols is few with a
247 really low $PM_{2.5}$ level in summer in Beijing. The sudden elevated ambient particle
248 concentration (Haze I and Haze II) brought the worst PM pollution in Beijing this
249 summer and has been widely concerned by the public. Thus, the formation mechanism
250 of Haze I and Haze II in which the concentrations of $PM_{2.5}$ and O_3 were
251 simultaneously/alternately high should be discussed systematically. The key point is to
252 determine the oxidation capacity of regional atmosphere and to clarify the formation
253 mechanism of secondary aerosols. Besides, the occurrence and evolution patterns of the

https://doi.org/10.5194/acp-2019-966
Preprint. Discussion started: 17 January 2020


Atmospheric Chemistry and Physics Discussions

two haze processes were different, which could refer to the diverse accumulation mechanism, regional transfer contribution, ABL structure, and removal process. So, by clarifying the various pollution processes, it is possible to conclude the leading factors of the haze phenomenon in Beijing in summer. In short, we are going to explore the causes of haze pollution under strong atmospheric oxidization capacity, in terms of the physics process such as sources and sinks of pollutants and ABL structure influence, and the chemistry process, which means aerosol transformation process.

3.2 The formation mechanism of haze pollution in summer in Beijing

https://doi.org/10.5194/acp-2019-966
Preprint. Discussion started: 17 January 2020

Atmospheric Chemistry and Physics Discussions

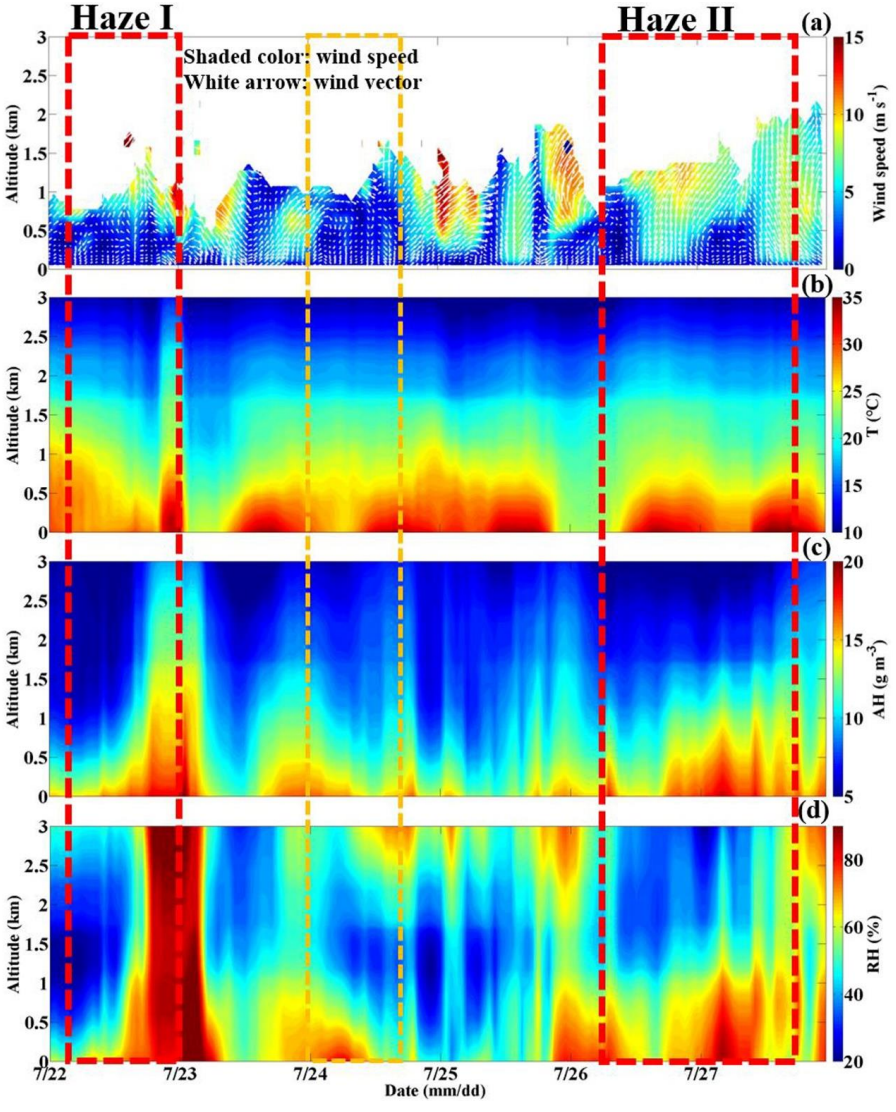

Figure 4. Temporal variation on vertical profiles of (a) horizontal wind vector (white arrows denote wind vectors), (b) temperature (T), (c) absolute humidity (AH), and (d) relative humidity (RH) in the BJ site during July 22-27, 2019. (The yellow-mark part represents the light haze pollution period and the red-mark part represents heavy haze pollution episode.)

https://doi.org/10.5194/acp-2019-966
Preprint. Discussion started: 17 January 2020

Atmospheric Chemistry and Physics Discussions

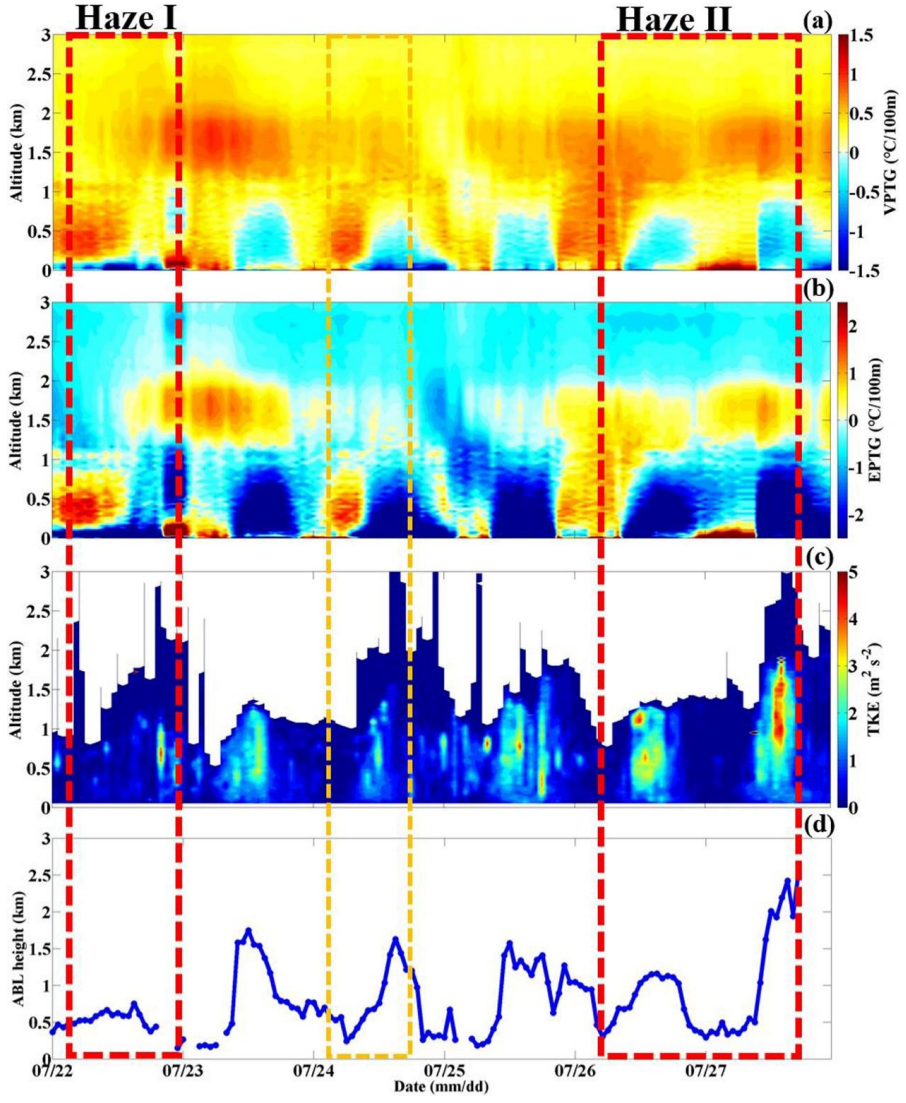

Figure 5. Temporal variation on vertical profiles of (a) virtual potential temperature gradient (VPTG: $\partial\theta_v/\partial z$), (b) pseudo-equivalent potential temperature gradient (EPTG: $\partial\theta_{se}/\partial z$) and (c) turbulent kinetic energy (TKE), along with corresponding (d) atmospheric boundary layer height (ABLH) in the BJ site during July 22-27, 2019. (The yellow-mark part represents the light haze pollution period and the red-mark part represents heavy haze pollution episode.)

https://doi.org/10.5194/acp-2019-966
Preprint. Discussion started: 17 January 2020

Atmospheric Chemistry and Physics Discussions

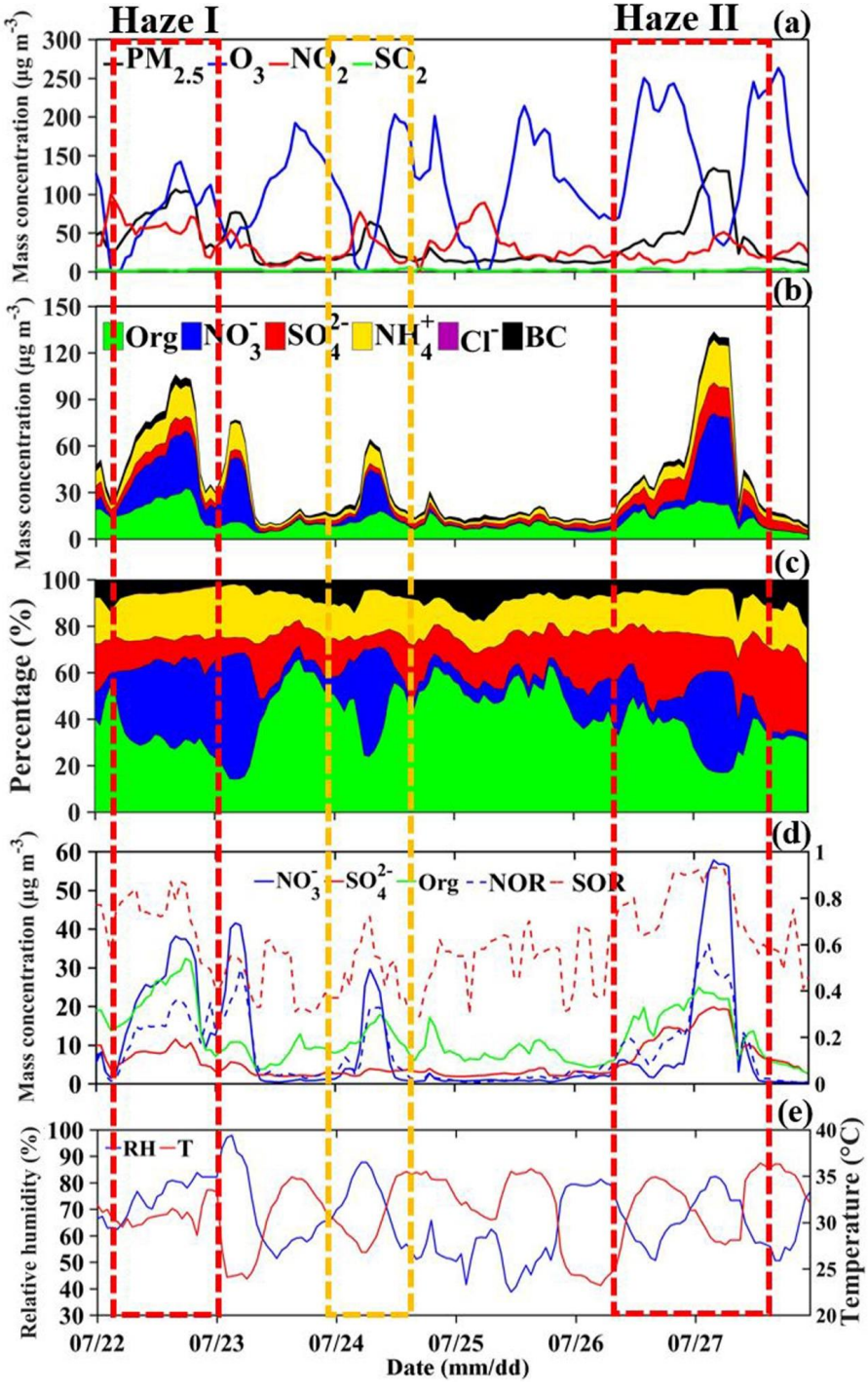

275

276 Figure 6. Temporal variation on mass concentrations of (a) $PM_{2.5}$, O_3, NO_2 as well as SO_2, (b)

https://doi.org/10.5194/acp-2019-966
Preprint. Discussion started: 17 January 2020


Atmospheric Chemistry and Physics Discussions

277 $PM_{2.5}$ chemical compositions, including Organics (Org), sulfate (SO_4^{2-}), nitrate (NO_3^-),
278 ammonium salt (NH_4^+), chlorine salt (Cl^-) and black carbon (BC) in the BJ site during July 22-
279 27, 2019. (c) Temporal variation on the relative contribution of chemical compositions to $PM_{2.5}$
280 mass concentration in the BJ site during July 22-27, 2019. (d) Temporal variation on mass
281 concentration of dominant $PM_{2.5}$ chemical compositions, sulfur oxidation ratio (SOR) and
282 nitrogen oxidation ratio (NOR) in the BJ site during July 22-27, 2019. (e) Temporal variation
283 on relative humidity (RH) and temperature (T) in the BJ site during July 22-27, 2019. (The
284 yellow-mark part represents the light haze pollution period and the red-mark part represents
285 heavy haze pollution episode.)

286 **3.2.1 The occurrence stage**

287 As shown in Fig. 3a, the PM levels in Beijing have been gradually increasing
288 from 8:00 to 22:00 on the 26th (Haze II) and from 4:00 to 22:00 on the 22nd (Haze I),
289 with $PM_{2.5}$ mass concentration eventually reaching 75 μg m^{-3} and 131 μg m^{-3},
290 respectively. The two stages were respectively regarded as the occurrence stages of
291 Haze I and Haze II.

292 ***a. The contribution of pollution transport***

293 Owing to the serious control measures in the summer of Beijing, the sudden
294 elevated PM levels were very likely to origin the outside region. It's clear that since the
295 wee hours on the 22nd and 26th, Beijing was located behind the northwest-southeast
296 trough of the 850-hPa potential height field, which bordered the Sichuan Basin to the
297 west (Fig. 7a-d; Fig. 7i-l). Based on it, Beijing was always under the control of strong
298 southerly winds at high altitudes. With Taihang mountains to the east and Yanshan
299 mountains to the north (Fig. 2), Beijing is in semi-enclosed terrain, thus, the south wind
300 belt passing through the north China plain to Beijing will be strengthened (Su et al.,
301 2004). The southerly wind speed respectively reached ~8-10 m s^{-1} (Haze II) and ~5-7
302 m s^{-1} (Haze I) at >0.5 km altitude. As the strong southerly winds persistently blew from
303 the south, the moisture transport channel, where the water vapor was carried to Beijing
304 under the southerly winds, was formed and became more and more significant (Fig. 7a-
305 d; Fig. 7i-l). In response, the humidity in Beijing showed a conspicuous increase in the

https://doi.org/10.5194/acp-2019-966
Preprint. Discussion started: 17 January 2020


Atmospheric Chemistry and Physics Discussions

306 morning of 26th with the AH (RH) reaching ~15-17 g m^{-3} (~75 %) while decreased from
307 10:00 with the AH (RH) down to ~13 g m^{-3} (~70 %) (Fig. 4c-d). The air temperature
308 during the daytime was extremely high reaching ~30-35 ℃ (Fig. 4b), and high-
309 temperature weather would reduce the humidity by the evaporation to some degree.
310 Considering air temperature was always at a distinctly high level (~30 ℃) since the
311 early morning of 22nd, the AH (RH) was ~13 g m^{-3} (~65 %) during the occurrence stage.
312 With the more populated industrial regions in the south of Beijing, strong winds
313 blowing from the south were also highly possible to transport heavy anthropogenic
314 aerosols to Beijing (Chang et al., 2018; Liu et al., 2013b). To explore the potential PM
315 transportation, we made the distribution maps of $PM_{2.5}$ mass concentration in most parts
316 of China (Fig. 8) and combined with the corresponding background circulation fields
317 to try illustrating the pollution transportation. The regional distribution of $PM_{2.5}$ mass
318 concentration was obtained by interpolating $PM_{2.5}$ data from more than 1000 stations
319 of China National Environmental Monitoring Centre into grid data (0.5°×0.5°). Noted
320 that at 2:00 of the 26th and 22nd, both the high $PM_{2.5}$ mass concentration (~70 μg m^{-3} for
321 Haze I and ~50 μg m^{-3} for Haze II) were mainly distributed in the south/southwest of
322 Beijing, dramatically higher than that (~10 μg m^{-3}) in Beijing city (Fig. 8a-b; Fig. 8i-l).
323 The south area of Beijing heavily polluted was mainly in Baoding, Langfang and
324 Shijiazhuang and so on, which are generally ~60-300 km far away from Beijing (Fig.
325 2). The southerly air mass above ~0.5 km moved more than ~20-30 km h^{-1} (estimated
326 from the measured wind speed) on the 26th and 22nd, which is fast enough to transport
327 pollutants to Beijing in several hours. As expected, the high $PM_{2.5}$ mass concentration
328 area gradually spread northward sensitively corresponding to the southerly winds, and
329 consequently, the highest $PM_{2.5}$ level located in Beijing at 20:00 on both the 26th
330 (reaching ~65 μg m^{-3}) and 22nd (reaching ~80 μg m^{-3}). It was consistent with the rising
331 trends of $PM_{2.5}$ in this time shown in Fig. 3a. The averaged rising rate of $PM_{2.5}$
332 concentration (~5.8 μg m^{-3} h^{-1}) on the 22nd was higher than that (~3.73 μg m^{-3} h^{-1}) on
333 the 26th, possibly related to the bigger difference of $PM_{2.5}$ concentration between
334 Beijing city and the south area of Beijing. The results were consistent with the findings

https://doi.org/10.5194/acp-2019-966
Preprint. Discussion started: 17 January 2020


Atmospheric Chemistry and Physics Discussions

335 reported in Zhong et al. (2018). Thus, multiple results implied that PM transportation
336 by southerly winds was primarily responsible for the PM rising in the occurrence stage.

337 ***b. The effect of atmospheric boundary layer structure***

338 As shown in Fig. 5a-b, in the forenoon of the 26th and 22nd, the positive values of
339 the virtual potential temperature gradient ($\partial\theta_v/\partial z$) and pseudo-equivalent potential
340 temperature gradient ($\partial\theta_{se}/\partial z$) at 0-2 km altitude (Haze II) and at 0-1 km altitude (Haze
341 I) indicated a stable atmosphere layer existing. Generally, with no solar radiation
342 reaching the ground and more upward long-wave radiation from the ground in the
343 nighttime, the surface is cooled faster than the upper atmosphere, promoting a stable
344 atmosphere. In response, the turbulent kinetic energy (TKE) was extremely low (0-1
345 $m^2\ s^{-2}$) along with a low ABLH of ~0.5 km (Fig. 5c-d). It means for both the 26th and
346 22nd, the south winds kept blowing when the ABL structures were not conducive to the
347 vertical diffusion of substances. The stable ABL structure suppressing the vertical
348 diffusion of pollution also to some degree contributed to the occurrence of PM pollution.
349 Both the $\partial\theta_v/\partial z$ and $\partial\theta_{se}/\partial z$ at 0-1.5 km altitude turned to negative at 14:00-16:00 on the
350 26th, indicating an unstable atmosphere layer. Generally, strong daytime solar radiation
351 reaching the surface may rebuild the vertical temperature structure and break the stable
352 ABL, especially in summer. Thus, the turbulence was quickly generated by
353 thermodynamic activity with TKE growing to ~2-3 $s^2\ m^{-2}$ and continued to develop
354 upwards causing ABLH gradually increased to ~1.2 km. This ABL process would
355 explain the slight fluctuations in the PM rising at this time in which the PM_{10} mass
356 concentration sharply decreased from 100 μg m^{-3} to 73 μg m^{-3}. Different from the ABL
357 condition on the 26th (Haze II), the $\partial\theta_{se}/\partial z$ was negative but the $\partial\theta_v/\partial z$ was positive
358 below ~1.5 km in the afternoon on the 22nd (Haze I). And combined with the low TKE
359 (~0-0.5 $m^2\ s^{-2}$) like that in the forenoon, the atmospheric stratification below ~1.5 km
360 was of absolutely stable state. Maybe little solar radiation heating the ground in the
361 afternoon on account of cloudy weather, the original stable ABL structure formed at
362 nighttime cannot be broken. All the above results imply that the ABL structure also
363 plays a role in the PM rising in the occurrence stage.

https://doi.org/10.5194/acp-2019-966
Preprint. Discussion started: 17 January 2020

Atmospheric Chemistry and Physics Discussions

c. The secondary aerosol formation driven by strong atmospheric oxidation capacity

When the $PM_{2.5}$ increased sensitively to strong southerly winds in Beijing during the occurrence stage in Haze II (Haze I), O_3 showed a sharper growth trend, increasing rapidly from 67 (26) μg m^{-3} and peaking at 250 (131) μg m^{-3}. As mentioned in section 3.1, the high concentration of O_3 indicates active atmospheric photochemical reactivity (Li et al., 2012; Seinfeld, 1986), thus, the atmosphere was of strong oxidizing capacity with the presence of large amounts of free radicals (OH, etc.) and ozone, which can promote the formation of secondary aerosols (Pathak et al., 2009; Shi et al., 2015; Wang et al., 2016). As seen in Fig. 6b, along with the increase in $PM_{2.5}$ concentration in this occurrence stage, the concentrations of organics, sulfate, and nitrate in $PM_{2.5}$ also gradually increased. The average concentrations of organics, sulfate, and nitrate in the occurrence stage of Haze II (Haze I) were 15.6 (23.0) μg m^{-3}, 10.0 (8.0) μg m^{-3} and 4.3 (24.7) μg m^{-3} and accounted for 40.7 (32.1) %, 25.3 (11.2) %, and 12.2 (31.5) % to $PM_{2.5}$ concentration, respectively. The total concentration of sulfate, organics, and nitrate (SON) accounted for more than 75 % to $PM_{2.5}$ concentration in the occurrence stage of both Haze II and Haze I (Fig. 6c), implying that the increase of SON is the leading cause of increase of $PM_{2.5}$ concentration. Secondary organics aerosols can be formed from the photochemical oxidation reactions of VOCs, emitted by vehicles (Hennigan et al., 2011). Thus, the high concentration and relative contribution of organics are mainly attributed to the active photochemical reactions in summer and huge vehicle emissions of VOCs in Beijing city. Due to the lack of VOCs data, the detailed formation mechanism of secondary organics would be further studied in the future. To explore the possible formation mechanism of secondary inorganic aerosols, sulfur oxidation ratio (SOR) and nitrogen oxidation ratio (NOR) respectively defined as $SOR = [SO_4^{2-}]/([SO_4^{2-}] + [SO_2])$ and $NOR = [NO_3^-]/([NO_3^-] + [NO_2])$, of which [ ] stands for the molar concentration were important and used in this paper. Higher SOR and NOR suggest the higher oxidation efficiency of sulfur and nitrogen, which means more secondary inorganic aerosols exist in the atmosphere (Liu et al., 2019c;

https://doi.org/10.5194/acp-2019-966
Preprint. Discussion started: 17 January 2020


Atmospheric Chemistry and Physics Discussions

Han et al., 2019; Yao et al., 2002; Kong et al., 2018; Sun et al., 2006).

Both homogeneous gas-phase and heterogeneous reactions can promote the formation of sulfate from SO_2 during haze episodes (Khoder, 2002; Harris et al., 2013), increasing the SOR. Noted that SOR values during the whole observation period (from the 22nd to the 27th) were relatively high, averaging 0.62, along with relatively low SO_2 level, averaging 2.2 μg m^{-3} (Fig. 6a; d). The observed high SOR values could be attributed to the relatively high RH (averaged ~66.6 %) (Fig. 6e) and ubiquitous photochemical reactions in summer in Beijing (Han et al., 2019). Nevertheless, compared to the quite low PM level in clean day (on the 25th) (Fig. 6d), the temporal variation of sulfate concentration on the 26th (Haze II) and 22nd (Haze I) showed a distinct increase trend in the occurrence stage, gradually increasing from 3.7 μg m^{-3} to 14.4 μg m^{-3} and from 4.2 μg m^{-3} to 11.5 μg m^{-3}, respectively. Meanwhile, SOR values also at higher level averaged ~0.76 in the occurrence stage of both Haze II and Haze I than those in clean day averaged ~0.55 (Fig. 6c). The results indicated an enhanced secondary sulfate aerosol formation in the occurrence stage. However, the PM level and sulfate concentration in clean day are quite low, but the concentration of O_3 is relatively high (Fig. 6a), reaching up to 214 μg m^{-3}, which means active photochemical reactions. Thus, although the significant photochemical reactions occurred at daytime on the 26th and 22nd facilitated the homogeneous gas-phase oxidation of SO_2 to a certain extent, but it is not the dominant reason for the increase of sulfate in the occurrence stage. Noted that the PM level and total chemical compositions mass slowly increased on the 24th with no pollution transportation by south winds (Fig. 3a-b; Fig. 7e-h; Fig. 8e-h;), while the averaged concentration of sulfate was 2.8 μg m^{-3} and only accounted for 10.7 %, far lower than those in Haze II and similar to those on the clean day. And the average RH was 61.4 % and 75.3 % in the occurrence stage of Haze II and Haze I, which also higher than that in the clean day (54.5 %). According to the results mentioned above, strong winds blowing from the south and southwest of Beijing bring numerous moisture and particles, we infer that the increase in sulfate aerosols in Haze II and Haze I could be mainly attributed to the regional transport, then the moisture and

https://doi.org/10.5194/acp-2019-966
Preprint. Discussion started: 17 January 2020


Atmospheric Chemistry and Physics Discussions

422 particles transported to Beijing further facilitated the heterogeneous reactions of SO_2
423 on moist aerosol surface. This highlights the importance and urgency of enhancing joint
424 regional pollution emission control.

425 Nitrate can be formed predominantly via both the homogeneous gas-phase
426 photochemical reaction of NO_2 with OH radical at daytime when photochemical
427 activity is high (Wang et al., 2006; Wen et al., 2018; Seinfeld and Pandis, 2006), and
428 heterogeneous hydrolysis reaction of NO_3 and N_2O_5 in the atmosphere during the
429 nighttime (Richards, 1983; Russell et al., 1986; Wang et al., 2009; Wang et al., 2017a;
430 Pathak et al., 2011). In addition, there is an equilibrium between particulate nitrate and
431 gaseous HNO_3 and NH_3 in the atmosphere due to ammonium nitrate is semi-volatile
432 (Seinfeld, 1986). High temperature could promote the decomposition of ammonium
433 nitrate, thus, the regional transport of ammonium nitrate in summer was not considered
434 (Li et al., 2019). As shown in Fig. 6b and d, the nitrate concentration (NOR) in the
435 occurrence stage of Haze II was lightly increased from 3.2 μg m^{-3} (0.09) at 8:00 to 5.2
436 μg m^{-3} (0.23) at 22:00. While the nitrate concentration (NOR) in the occurrence stage
437 of Haze I sharply increased from 2.7 μg m^{-3} (0.02) at 8:00 to 38.1 μg m^{-3} (0.36) at 16:00.
438 The concentration of nitrate and relative contribution of nitrate to PM during Haze I
439 were markedly higher than those in Haze II (Fig. 6c). This inconsistency could be
440 attributed to the high temperature (averaging ~34 ℃) in Haze II than that (averaging
441 ~27 ℃) in Haze I (Fig. 6e). These results indicated that strong photochemical reactions
442 can facilitate the formation of nitrates, increasing the $PM_{2.5}$ level, while the nitrate
443 would be decomposed into gaseous HNO_3 and NH_3 once the temperature is high. After
444 15:00, the concentration of nitrates began to increase for the presence of large amounts
445 of radicals and dropped temperature inhibited the reverse reaction. Into the night, the
446 increase of nitrate aerosols was predominantly through heterogeneous hydrolysis
447 reaction of NO_3 and N_2O_5 in the atmosphere, more details would be discussed in the
448 next section.

449 **3.2.2 The outbreak stage**

450 The $PM_{2.5}$ mass concentration suddenly increased from 75 μg m^{-3} at 22:00 on the

https://doi.org/10.5194/acp-2019-966
Preprint. Discussion started: 17 January 2020


Atmospheric Chemistry and Physics Discussions

451 26^{th} to 146 μg m^{-3} at 4:00 on the 27^{th} and stayed high values of ~150 μg m^{-3} until 10:00,
452 which was identified as an outbreak stage of haze pollution (Fig. 3a). Comparing to
453 the atmospheric BSC of ~2.5-3 M $m^{-1}sr^{-1}$ on the 26^{th}, the ambient particles
454 concentrated below ~0.5 km altitude with a sharply increased atmospheric scattering
455 coefficient, reaching more than 6 M $m^{-1}sr^{-1}$ (Fig. 3b).

456 ***a. The contribution of southerly transport was almost gone***

457 There were still strong southerly winds controlling Beijing at high altitude (>0.5
458 km), accompanied by a more significant vapor transportation channel under it (Fig.
459 7m-n). However, PM levels in the south/southeast of Beijing, ranging from 0 to ~60
460 μg m^{-3}, were significantly lower than that (>80 μg m^{-3}) in Beijing, even below air
461 quality standards (Fig. 8n-m). It's not likely to make an explosive growth of PM level
462 and maintain a high PM level in Beijing by pollution transportation.

463 ***b. Extremely stable ABL structure was the prerequisite for pollution outbreak***

464 Without the effect of pollution transportation, more attention was paid to the
465 interior of the local ABL, and Fig. 5 exhibited the temporal variation of the ABL
466 structure. Both the values of $\partial\theta_v/\partial z$ and $\partial\theta_{se}/\partial z$ turned to positive (~1.5 ℃/100 m and
467 ~2.5 ℃/100 m, respectively) below ~0.3 km altitude, as depicted in Fig. 5a-b. It
468 implied a very stable lower layer defined as nocturnal stable boundary layer (NSBL)
469 was formed with ABLH of ~0.3 km. By the strong radiation effect of already-existing
470 high aerosol loading at daytime, the surface solar radiation could be strongly blocked
471 and reduced, conducive to a stable stratification formed at midnight (Zhao et al., 2019;
472 Zhong et al., 2017). In such a thermally stable state, the buoyancy transport heat flux
473 in the atmosphere will continuously consume turbulent energy, suppressing the
474 development of turbulence. Therefore, the corresponding TKE was in a sharp decrease
475 compared to that in 14:00-16:00 on the 26^{th}, lower than ~0.5 m^2 s^{-2} even near to ~0 m^2
476 s^{-2} (Fig. 5c-d). However, the values of $\partial\theta_v/\partial z$ and $\partial\theta_{se}/\partial z$ were respectively positive
477 and negative from ~0.3 km to ~1.5 km, which means this atmospheric layer was of
478 conditional instability. Considering the quite low TKE like that below ~0.3 km, this
479 layer recognized as the residual layer was also absolutely stable. Thus, the ambient

https://doi.org/10.5194/acp-2019-966
Preprint. Discussion started: 17 January 2020


Atmospheric Chemistry and Physics Discussions

particles were restrained from vertically spreading and concentrated below the NSBL, leading to a growth of the ground PM level. The same work would happen to the ambient water vapor transported by the southerly winds, which explained the extremely high humidity during this period. As shown in Fig. 4c-d, the atmospheric humidity in the outbreak stage was distinctly higher than that on the 26th with the AH (RH) reaching ~20 g m^{-3} (~90 %). Different from the role of moisture transport channel, the unique NSBL structure has a more significant impact on the increase of air humidity.

In contrast, for the Haze I on the 22nd, there was no such thing as an outbreak stage of PM pollution, as the $PM_{2.5}$ mass concentration had sharply decreased from 131 μg m^{-3} to 53 μg m^{-3} in one hour since 21:00. The reason that the ambient particles were not accumulated and maintain high level like that in Haze II was the ABL structure has not met the similar characteristics. The already-existing high $PM_{2.5}$ level (~130 μg m^{-3}) at daytime would accelerate the surface cooling causing the NSBL formed more easily with a very low height of ~0.2 km. This situation was similar to that in Haze II. Nevertheless, the TKE above the NSBL was very high reaching ~2-3 m^2 s^{-2}, in notable contrast to that in Haze II where the TKE was extremely low (~0 m^2 s^{-2}) in the whole 0-1.5 km layer. The vertical temperature structures above the NSBL meant the atmosphere was of conditional instability, while in terms of the TKE distribution, the atmospheric stratification above the NSBL in Haze I was unstable, in contrast to the stable one in Haze II. Because it was raining at night with the high AH (~15-20 g m^{-3}) and RH (>90 %) extending from surface to ~3 km altitude, the convection activity was quite strong accompanied by a wet deposition process. Due to the unstable ABL structure and the accompanying wet deposition, the ambient particle concentration cannot explosively increase but instead was removed from the atmosphere.

Noted that the PM on the 24th also showed a tendency to increase, but it suddenly reduced like that in Haze I. There was no transportation effect contributing to the increase of PM level on the 24th with westerly circulation field controlling (Fig. 7e-h).

https://doi.org/10.5194/acp-2019-966
Preprint. Discussion started: 17 January 2020


Atmospheric Chemistry and Physics Discussions

Similar to the occurrence stages in Haze I and Haze II, a stable atmosphere near the surface was formed with the positive $\partial\theta_v/\partial z$ and $\partial\theta_{se}/\partial z$. Under these stable stratifications, the PM from local emission on the 24th started increasing. By the strong daytime solar radiation heating the surface quickly, it may break up the anomalous vertical temperature structures formed by long-wave radiation cooling at nighttime and changed them into the unstable stratifications with negative $\partial\theta_{se}/\partial z$ ($\partial\theta_v/\partial z$) profiles. As discussed in Haze II, the ABL structure characterized by increased TKE (~2-3 m^2 s^{-2}) and elevated ABLH (~1.5 km) would dissipate the pollution soon. However, the difference between the Haze II and the pollution process on the 24th was that the unstable atmospheric stratifications with strong TKE on the 24th kept developing until the end of the day, while for Haze II, this condition just lasted two or three hours at noon. Additionally, an NSBL formed at midnight in Haze II with the ABL height of ~0.3 km, making the vertical diffusion condition in the near stratum even worse. Therefore, the subsequent stable atmospheric stratification on the 26th was the necessary premise for the pollution outbreak in Haze II. Particles would not be accumulated and lead to an outbreak of pollution without a stable ABL structure and can be easily dissipated by the self-cleaning capacity of the atmosphere.

c. Intense secondary aerosol formation driven by atmospheric oxidation capacity drove the pollution outbreak

Heterogeneous aqueous reactions reference to the secondary formation of sulfates and nitrates largely related to ambient humidity (Wang et al., 2012; Gibson et al., 2007). The accumulation of water vapor in the NSBL would facility the formation of secondary aerosols and further driven the outbreak of PM pollution. In order to investigate the explosive growth mechanisms, we divided the outbreak stage of PM pollution during Haze II into two stages: Stage I, from 22:00 on the 26th to 4:00 on the 27th; Stage II, from 5:00 to 10:00 on the 27th. During Stage I, along with the explosive growth of $PM_{2.5}$, the concentration of nitrate rapidly increased from 11.6 μg m^{-3} to 57.8 μg m^{-3}, while sulfate and organics sightly increased from 13.7 μg m^{-3} to 19.8 μg m^{-3} and from 21.8 μg m^{-3} to 24.9 μg m^{-3} (Fig. 6d), respectively. During Stage II, the nitrate

https://doi.org/10.5194/acp-2019-966
Preprint. Discussion started: 17 January 2020


Atmospheric Chemistry and Physics Discussions

concentration stayed the highest value of ~57 μg m^{-3} and the sulfate level maintained ~19 μg m^{-3}, with organics slowly dropping (Fig. 6d). The explosive growth trend of nitrate is the most consistent with that of $PM_{2.5}$. In addition, the average concentrations of organics, sulfate, and nitrate in the whole outbreak stage were 20.6 μg m^{-3}, 15.9 μg m^{-3} and 43.0 μg m^{-3} and accounted for 22.0 %, 17.8 %, 34.9 %, respectively. Compared to the occurrence stage, the relative contribution of organics and sulfate to $PM_{2.5}$ decreased significantly, while the contribution of nitrate obviously increased. These results indicated that the explosive growth of $PM_{2.5}$ concentration was driven by the sharp increase in nitrate concentration. With strong photochemical reactions at daytime, the mass concentration of O_3 was very high before the outbreak stage, up to 214 μg m^{-3}. NO_2 would be produced by O_3 reacting with a large amount of NO which was discharged by vehicle in the evening peak. While NO_2 would react with O_3 aloft to form NO_3 which will rapidly react with NO_2 to form N_2O_5 at nighttime. During stage I, NOR rapidly increased from 0.26 to 0.60, which implied the oxidization rate of NO_2 sharply increased in a few hours. Considering NO_2 stayed relative low value of ~25 μg m^{-3} and O_3 rapidly decreased from 214 μg m^{-3} to 46 μg m^{-3} in stage I (Fig. 6a), the consumption process of NO_2 was more significant than the generation process. The NO_2 produced by consuming O_3 was constantly oxidized by O_3 to produce a large amount of N_2O_5, resulting in a sharp decline in O_3 concentration. Once N_2O_5 was produced, it would absorb on the moist particle surfaces and react with water in droplets to form nitrate, resulting in a sudden increase in nitrate, from 11.6 μg m^{-3} to 57.8 μg m^{-3}. During Stage II, O_3 slowly decreased to 34 μg m^{-3} at 6:00 on the 27th and NO_2 stayed relatively high value (~44-51 μg m^{-3}), which meant the generation process of NO_2 was dominated. Thus, the oxidization of NO_2 was not further increasing with the NOR maintaining ~0.45 during Stage II. Then, the nitrate, formed by the pathway that N_2O_5 adsorbed on surfaces and reacts with water in droplets, did not increase anymore, maintaining the highest mass concentration of ~57 μg m^{-3}. The processes mentioned above were unimportant at daytime because N_2O_5 was in equilibrium with NO_3, that is, NO_3 was photolyzed as well as rapidly destroyed by NO which in turn was present whenever

https://doi.org/10.5194/acp-2019-966
Preprint. Discussion started: 17 January 2020


Atmospheric Chemistry and Physics Discussions

there were NO_x and sunlight. During both Stage I and Stage II, SOR always maintained a relatively high level of ~0.95, accompanied by a high RH of ~90 %. High SOR and RH signified that the heterogeneous reaction dominated the formation of particulate sulfate during the outbreak stage. The increased amount of sulfate lower than nitrate may relate to the few emissions of SO_2 and massive emission of NO from vast vehicles. This highlights the importance and urgency of enhancing NOx (vehicles) emission control.

Contrary to expectations, after the wet deposition process in Haze I, the concentrations of $PM_{2.5}$, NO_2 and the total chemical composition abruptly increased at 0:00 on the 23rd, accompanied by a sharp increase of nitrate and NOR (from 9.3 μg m^{-3} to 41.5 μg m^{-3} and 0.26 to 0.49, respectively). These results may be related to the high RH (more than 93 %), which facilitated the heterogeneous hydrolysis reaction of NO_3 and N_2O_5, formed by gas pollutants on NOx and O_3 that wet deposition process did not completely clear.

3.2.3 The diffusion stage

Since 10:00 on the 27th, the $PM_{2.5}$ mass concentration had sharply reduced to 50 μg m^{-3} in three hours, during which the atmospheric BSC down to $<1\times10^3$ M m^{-1}sr^{-1} on the whole ABL (Fig.3 and Fig. 8o-p). It represented a stage of pollution diffusion. As no wet deposition process existed, the diffusion stage of Haze II was different from that of Haze I. Generally, the arrival of strong and clean air mass from the south is the main factor that dissipates the air pollution in Beijing (Zhong et al., 2017; Zhong et al., 2018; Zhao et al., 2019). Calm/light winds in the lower layer were dominated in the outbreak stage, while sudden increased southerly winds blew in the 0-2 km layer since 8:00 on the 27th, with a wind speed of ~6-9 m s^{-1} (Fig. 7n-q and Fig. 4a). Strong winds would play a role in the horizontal diffusion of the accumulated PM at surface. Then, accompanied by the horizontal diffusion, the strong solar radiation at noon reached the surface and changed the vertical temperature structure. The ABL was in extremely unstable state for both the $\partial\theta_v/\partial z$ and $\partial\theta_{se}/\partial z$ were negative below ~1.0 km with values of -0.5 ℃/100 m and -2.5 ℃/100 m, respectively (Fig. 5a-b). Along with the instability,

https://doi.org/10.5194/acp-2019-966
Preprint. Discussion started: 17 January 2020


Atmospheric Chemistry and Physics Discussions

596 the development of turbulence in the ABL was very strong and quick, with the TKE
597 values suddenly increasing to ~3-5 $m^2 s^{-2}$ (Fig. 5c). Accompanied by the pronounced
598 turbulence development, the ABL continuously developed upward with the ABLH up
599 to the ~2.5 km in short time (Fig. 5d). The ABL structure quickly became extremely
600 suitable for the vertical diffusion of pollutants, thus, the PM level sharply decreased
601 during this time.

602 Different from $PM_{2.5}$, the concentration of O_3 rapidly increased due to the
603 increasing radiation, along with the high concentrations of NO_2 and NO attributed to
604 morning traffic emissions. Along with the decline in $PM_{2.5}$, organics, and sulfate slowly
605 decreased to less than ~3 μg m^{-3} and nitrate reduced to below 1.0 μg m^{-3}. The average
606 concentrations of organics, sulfate, and nitrate were down to 6.8 μg m^{-3}, 6.2 μg m^{-3} and
607 1.9 μg m^{-3} and accounted for 33.0 %, 32.3 %, 6.0 %, respectively. As significant
608 turbulence activity made vertical transportation of vapor, heat, and particles and so on,
609 the RH decreased to ~60 % accompanied by a decline in SOR (~0.75). This emphasized
610 the strong correlation between humidity and the heterogeneous formation mechanism
611 of sulfate. In addition, NOR rapidly decreased from 0.22 to 0.01, coincide with the
612 variation of nitrate. At this stage, temperature always maintained a high level of ~35 ℃.
613 Thus, similar to the situation in the occurrence stage, ammonium nitrate evaporated
614 under the high temperature, contributing to a decline in nitrate. In short, during the
615 diffusion stage, the unstable ABL structure was not only conducive to the diffusion of
616 pollution but also changed the T and RH, so as to inhibit the formation of secondary
617 aerosols and further reduce the secondary aerosols.

618 No matter the wet deposition in Haze I or the vertical diffusion in Haze II,
619 eventually, the air pollution would be cleared as long as the atmosphere of a specific
620 state. In other words, it implies that the self-cleaning capacity of the atmosphere is
621 responsible for the dispersion of air pollution. When the atmosphere is in what state can
622 the self-cleaning capacity of the atmosphere come into play so that the pollution can be
623 removed from the atmosphere. To discuss it, the key factors characterizing the self-
624 cleaning capacity of the atmosphere should be found out first. As analyzed above, once

https://doi.org/10.5194/acp-2019-966
Preprint. Discussion started: 17 January 2020

Atmospheric Chemistry and Physics Discussions

the TKE increased to >1.5-2 $m^2 s^{-2}$, the ABLH grew to more than ~1 km, and the $\partial\theta_v/\partial z$ & $\partial\theta_{se}/\partial z$ turned to negative, as well as no calm/light winds, the atmosphere was in a state of instability with strong turbulence activities and advection transport, and air pollution was spread away immediately. Owing to limited observation time, the results about the characteristics of self-cleaning capacity of the atmosphere may be not universal, and more comprehensive discussions on the self-cleaning capacity of the atmosphere would be studied in the future.

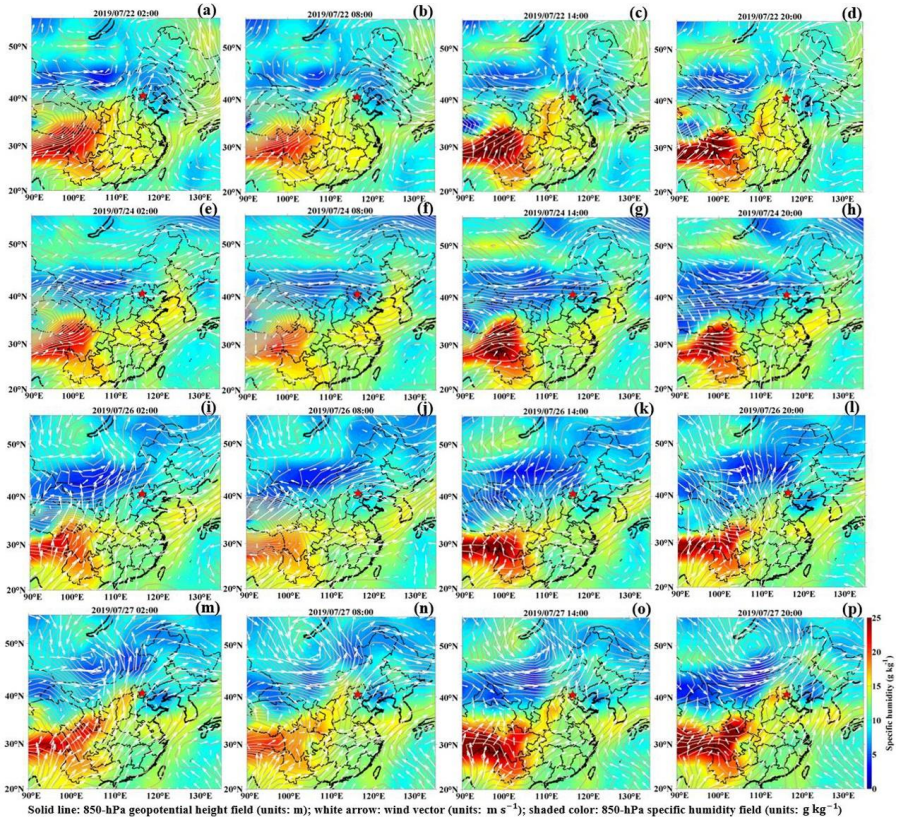

Figure 7. Composites of the 850-hPa horizontal wind vector field (units: m s^{-1}, white arrows), 850-hPa geopotential height field (units: m, solid lines) and 850-hPa specific humidity field (units: g kg^{-1}, shaded colors) at 0200, 0800, 1400, and 2000 (LT) on July 22, 24 and 26-27, labeled as (a) - (p). The star shows the location of the BJ site.

https://doi.org/10.5194/acp-2019-966
Preprint. Discussion started: 17 January 2020

Atmospheric Chemistry and Physics Discussions

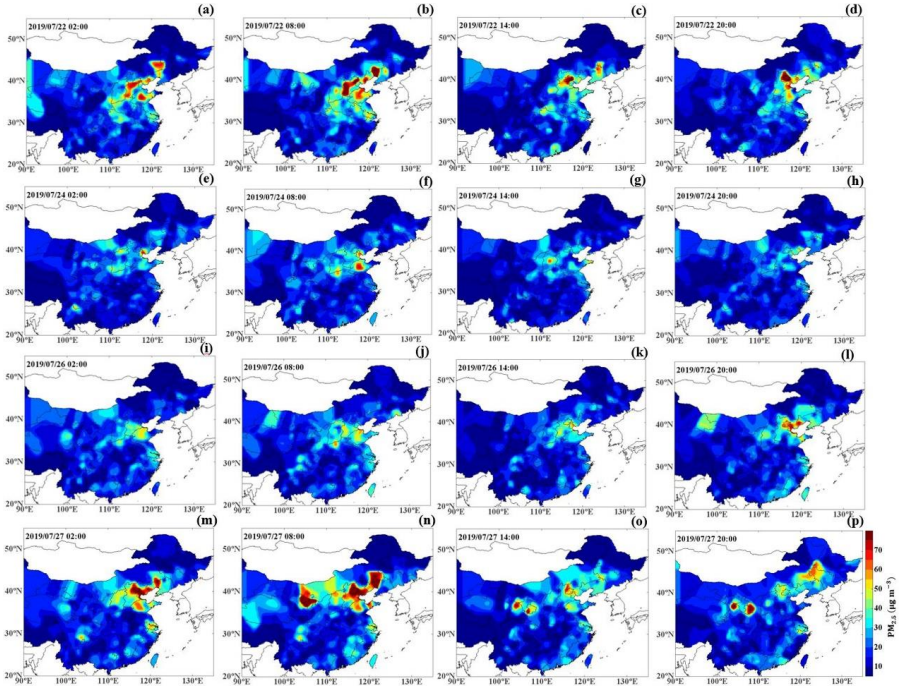

Figure 8. The $PM_{2.5}$ mass concentration distribution (units: μg m^{-3}, shaded colors) over most of China at 0200, 0800, 1400, and 2000 (LT) on July 22, 24 and 26–27, labeled as (a)–(p).

4 Conclusion

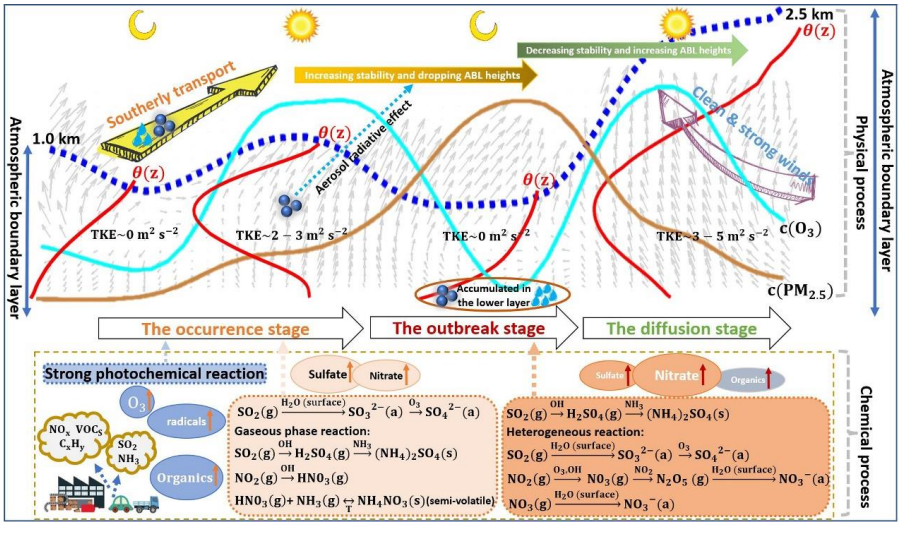

Figure 9. A schematic diagram for the formation mechanism of haze pollution under strong atmospheric oxidization capacity in summer in Beijing.

https://doi.org/10.5194/acp-2019-966
Preprint. Discussion started: 17 January 2020


Atmospheric Chemistry and Physics Discussions

The extremely serious haze pollution episode characterized by alternate/synchronous heavy PM loading and high ozone concentration occurred this summer in Beijing. Combined with a series of observations, the formation mechanism of haze pollution under strong atmospheric oxidization capacity has been deeply and systematically analyzed in terms of atmospheric physical process and chemical process.

The occurrence of haze pollution in summer in Beijing was mainly attributed to southerly transport and affected by the ABL structure to some degree (physical process), which was further promoted by the intense secondary aerosol formation with strong atmospheric oxidation capacity (chemical process). On the one hand, the physical process, where large amounts of moisture and particles were transported to Beijing under strong southerly winds, caused the initiation of haze pollution in Beijing. Moreover, it occurred when the ABL structure was extremely stable with low TKE and positive potential temperature gradient ($\partial\theta/\partial z$), facilitating the PM level rising in Beijing. And the stable ABL was broken and transformed into unstable (negative $\partial\theta/\partial z$) with strong solar radiation in the afternoon, responsible for the fluctuation of the PM rising process. On the other hand, the moisture and particles transported to Beijing further facilitated the heterogeneous reactions of SO_2 on moist aerosol surfaces. And for the significant photochemical reaction, the concentration of O_3 was quite high at daytime and the atmosphere was of strong oxidation capacity with large amounts of radicals (OH, etc.) and O_3, promoting the formation of secondary aerosols (sulfate, nitrate, and organics). Even so, the distinct increase in sulfate concentration was mainly linked by southerly transport, which carried heavy sulfate aerosol loading to Beijing. The physical process, where extremely stable ABL inhibited the diffusion of PM and moisture making an accumulation of ambient humidity and ground-level $PM_{2.5}$, was the premise of the outbreak of haze pollution. Under stable ABL, the formation of secondary aerosols dominated by nitrate was quite intense, and this pronounced chemical process was the key driving force leading to pollution outbreak. PM levels in the south/southeast of Beijing were significantly lower than that in Beijing, even below air quality standards. The contribution of pollution transportation was not important.

https://doi.org/10.5194/acp-2019-966
Preprint. Discussion started: 17 January 2020


Atmospheric Chemistry and Physics Discussions

Owing to the already-existing high $PM_{2.5}$ level at daytime, strong aerosol radiation effect would cool the surface and heat the above layer, facilitated the formation of the nocturnal stable boundary layer (NSBL). The $\partial\theta/\partial z$ in the NSBL turned to positive increasing the atmosphere stability, dropping the ABLH and decreasing the TKE. The ambient particles & moisture were restrained from vertically spreading and concentrated below the NSBL, resulting in an elevated PM & humidity levels at surface. Due to the high level of O_3 produced by strong photochemical reactions at daytime and NOx discharged by vehicle in the evening peak, vast N_2O_5 and NO_3 were formed with a sharp increase of NOR. The heterogeneous hydrolysis reactions of N_2O_5 and NO_3 at the moist particle surface were very significant under quite high humidity. It resulted in the formation of numerous nitrate, which was the main cause of the explosive growth of $PM_{2.5}$ levels in the outbreak stage. More controls should be made to reduce NOx emissions and atmospheric oxidization capacity, such as strengthening the supervision of heavy diesel vehicles and collaborative control of NOx and VOCs, and continuously deepen regional joint control of air pollution. As PM level gradually increasing, a wet deposition process and an extremely unstable ABL structure respectively appeared on the 22nd (Haze I) and 24th, the ambient particles experienced a sharp decline before the outbreak stage. It emphasized that the ABL structure extremely restrained the diffusion of substances was a prerequisite for the pollution outbreak. With clean & strong winds passing through Beijing, the ABL changed to unstable with negative $\partial\theta/\partial z$ and increased ABLH. The strong turbulence activity promoted pollution diffusion. No matter the wet deposition process or the strong turbulence activity, eventually, the air pollution would be cleared as long as the atmosphere was of a specific state. The self-cleaning capacity of the atmosphere is responsible for the dispersion of air pollution. When the atmosphere is in what state can the self-cleaning capacity of the atmosphere comes into play is worthy of further study.

Data availability.

The surface $PM_{2.5}$ & PM_{10} and other trace gases observation data used in this study can be accessed from http://106.37.208.233:20035/. Atmospheric reanalysis data was

https://doi.org/10.5194/acp-2019-966
Preprint. Discussion started: 17 January 2020


Atmospheric Chemistry and Physics Discussions

obtained from the National Centers for Environmental Prediction (NCEP) (https://www.esrl.noaa.gov/psd/data/). Other datasets can be accessed upon request to the corresponding author.

Author contribution

ZD and LG performed the research and wrote the paper, contributing equally to this study. XJ, QJ, WY and WX provided writing guidance, revised and polished the paper. LZ, TG, HB and WL designed the experiments and DL, MY, WX and WF carried them out. GC contributed to discussions of results. All the authors have made substantial contributions to the work reported in the manuscript.

Competing interests.

The authors declare that they have no conflict of interest.

Acknowledgments

This study was supported by the Ministry of Science and Technology of China (grant number 2016YFC0202001), the CAS Strategic Priority Research Program (XDA23020301) and the National Natural Science Foundation of China (grant number 41375036). The authors are grateful for services rendered by the National Oceanic and Atmospheric Administration (NOAA) and National Centers for Environmental Prediction (NCEP). The authors are thankful for the data support from the National Earth System Science Data Sharing Infrastructure, National Science & Technology Infrastructure of China (available at http://www.geodata.cn).

References

Ainsworth, E. A., Yendrek, C. R., Sitch, S., Collins, W. J., and Emberson, L. D.: The Effects of Tropospheric Ozone on Net Primary Productivity and Implications for Climate Change, in: Annual Review of Plant Biology, Vol 63, edited by: Merchant, S. S., Annual Review of Plant Biology, 637-661, 2012.

Anger, A., Dessens, O., Xi, F., Barker, T., and Wu, R.: China's air pollution reduction efforts may result in an increase in surface ozone levels in highly polluted areas, Ambio, 45, 254-265, https://doi.org/10.1007/s13280-015-0700-6, 2016.

Banta, R. M., Pichugina, Y. L., and Brewer, W. A.: Turbulent velocity-variance profiles in the stable

https://doi.org/10.5194/acp-2019-966
Preprint. Discussion started: 17 January 2020

732 boundary layer generated by a nocturnal low-level jet, J. Atmos. Sci., 63, 2700-2719,
733 https://doi.org/10.1175/jas3776.1, 2006.
734 Bi, J., Huang, J., Shi, J., Hu, Z., Zhou, T., Zhang, G., Huang, Z., Wang, X., and Jin, H.: Measurement of
735 scattering and absorption properties of dust aerosol in a Gobi farmland region of northwestern China - a
736 potential anthropogenic influence, Atmos. Chem. Phys., 17, 7775-7792, https://doi.org/10.5194/acp-17-
737 7775-2017, 2017.
738 Chang, X., Wang, S., Zhao, B., Cai, S., and Hao, J.: Assessment of inter-city transport of particulate
739 matter in the Beijing-Tianjin-Hebei region, Atmos. Chem. Phys., 18, 4843-4858,
740 https://doi.org/10.5194/acp-18-4843-2018, 2018.
741 Chen, L., Guo, B., Huang, J., He, J., Wang, H., Zhang, S., and Chen, S. X.: Assessing air-quality in
742 Beijing-Tianjin-Hebei region: The method and mixed tales of PM2.5 and O-3, Atmos. Environ., 193,
743 290-301, https://doi.org/10.1016/j.atmosenv.2018.08.047, 2018.
744 Chen, Z., Chen, D., Wen, W., Zhuang, Y., Kwan, M. P., Chen, B., Zhao, B., Yang, L., Gao, B., Li, R., and
745 Xu, B.: Evaluating the "2+26" regional strategy for air quality improvement during two air pollution
746 alerts in Beijing: variations in PM2.5 concentrations, source apportionment, and the relative contribution
747 of local emission and regional transport, Atmos. Chem. Phys., 19, 6879-6891,
748 https://doi.org/10.5194/acp-19-6879-2019, 2019.
749 Cheng, J., Su, J., Cui, T., Li, X., Dong, X., Sun, F., Yang, Y., Tong, D., Zheng, Y., Li, Y., Li, J., Zhang,
750 Q., and He, K.: Dominant role of emission reduction in PM2.5 air quality improvement in Beijing during
751 2013-2017: a model-based decomposition analysis, Atmos. Chem. Phys., 19, 6125-6146,
752 https://doi.org/10.5194/acp-19-6125-2019, 2019a.
753 Cheng, N., Li, R., Xu, C., Chen, Z., Chen, D., Meng, F., Cheng, B., Ma, Z., Zhuang, Y., He, B., and Gao,
754 B.: Ground ozone variations at an urban and a rural station in Beijing from 2006 to 2017: Trend,
755 meteorological influences and formation regimes, J. Cleaner Prod., 235, 11-20,
756 https://doi.org/10.1016/j.jclepro.2019.06.204, 2019b.
757 Dickerson, R. R., Kondragunta, S., Stenchikov, G., Civerolo, K. L., Doddridge, B. G., and Holben, B.
758 N.: The impact of aerosols on solar ultraviolet radiation and photochemical smog, Science, 278, 827-830,
759 https://doi.org/10.1126/science.278.5339.827, 1997.
760 Ding, A., Huang, X., Nie, W., Chi, X., Xu, Z., Zheng, L., Xu, Z., Xie, Y., Qi, X., Shen, Y., Sun, P., Wang,

https://doi.org/10.5194/acp-2019-966
Preprint. Discussion started: 17 January 2020

J., Wang, L., Sun, J., Yang, X.-q., Qin, W., Zhang, X., Cheng, W., Liu, W., Pan, L., and Fu, C.: Significant reduction of PM2.5 in eastern China due to regional-scale emission control: evidence from SORPES in 2011–2018, Atmos. Chem. Phys., 19, 11791–11801, https://doi.org/https://doi.org/10.5194/acp-19-11791-2019., 2019.

Frischer, T., Studnicka, M., Gartner, C., Tauber, E., Horak, F., Veiter, A., Spengler, J., Kuhr, J., and Urbanek, R.: Lung function growth and ambient ozone - A three-year population study in school children, Am. J. Resp. Cirt. Care, 160, 390-396, https://doi.org/10.1164/ajrccm.160.2.9809075, 1999.

Gibson, E. R., Liu, Y., Cain, J. P., Wang, H., Grassian, V. H., Laskin, A., and Laskin, A.: Chemical Transformation of CaCO3 Particles by Heterogeneous Reaction with HNO3: Kinetic Measurements over a Wide Range of Humidity, American Geophysical Union, 2007.

Gregory, L.: Cimel Sunphotometer (CSPHOT) Handbook, Office of Scientific & Technical Information Technical Reports, 2011.

Han, L., Xiang, X., Zhang, H., Cheng, S., Wang, H., Wei, W., Wang, H., and Lang, J.: Insights into submicron particulate evolution, sources and influences on haze pollution in Beijing, China, Atmos. Environ., 201, 360-368, https://doi.org/10.1016/j.atmosenv.2018.12.045, 2019.

Harris, E., Sinha, B., van Pinxteren, D., Tilgner, A., Fomba, K. W., Schneider, J., Roth, A., Gnauk, T., Fahlbusch, B., Mertes, S., Lee, T., Collett, J., Foley, S., Borrmann, S., Hoppe, P., and Herrmann, H.: Enhanced Role of Transition Metal Ion Catalysis During In-Cloud Oxidation of SO2, Science, 340, 727-730, https://doi.org/10.1126/science.1230911, 2013.

Hassan, I. A., Basahi, J. M., Ismail, I. M., and Habeebullah, T. M.: Spatial Distribution and Temporal Variation in Ambient Ozone and Its Associated NOx in the Atmosphere of Jeddah City, Saudi Arabia, Aerosol Air. Qual. Res, 13, 1712-1722, https://doi.org/10.4209/aaqr.2013.01.0007, 2013.

He, S., and Carmichael, G. R.: Sensitivity of photolysis rates and ozone production in the troposphere to aerosol properties, J. Geophys. Res.: Atmos., 104, 26307-26324, https://doi.org/10.1029/1999jd900789, 1999.

Hennigan, C. J., Miracolo, M. A., Engelhart, G. J., May, A. A., Presto, A. A., Lee, T., Sullivan, A. P., McMeeking, G. R., Coe, H., Wold, C. E., Hao, W. M., Gilman, J. B., Kuster, W. C., de Gouw, J., Schichtel, B. A., Collett, J. L., Jr., Kreidenweis, S. M., and Robinson, A. L.: Chemical and physical transformations of organic aerosol from the photo-oxidation of open biomass burning emissions in an environmental

https://doi.org/10.5194/acp-2019-966
Preprint. Discussion started: 17 January 2020


Atmospheric Chemistry and Physics Discussions

790 chamber, Atmos. Chem. Phys., 11, 7669-7686, https://doi.org/10.5194/acp-11-7669-2011, 2011.
791 Huang, X., Liu, Z., Liu, J., Hu, B., Wen, T., Tang, G., Zhang, J., Wu, F., Ji, D., Wang, L., and Wang, Y.:
792 Chemical characterization and source identification of PM2.(5) at multiple sites in the Beijing-Tianjin-
793 Hebei region, China, Atmos. Chem. Phys., 17, 12941-12962, https://doi.org/10.5194/acp-17-12941-2017,
794 2017.
795 Khoder, M. I.: Atmospheric conversion of sulfur dioxide to particulate sulfate and nitrogen dioxide to
796 particulate nitrate and gaseous nitric acid in an urban area, Chemosphere, 49, 675-684,
797 https://doi.org/10.1016/s0045-6535(02)00391-0, 2002.
798 Kong, L., Du, C., Zhanzakova, A., Cheng, T., Yang, X., Wang, L., Fu, H., Chen, J., and Zhang, S.: Trends
799 in heterogeneous aqueous reaction in continuous haze episodes in suburban Shanghai: An in-depth case
800 study, Sci. Total Environ., 634, 1192-1204, https://doi.org/10.1016/j.scitotenv.2018.04.086, 2018.
801 Li, L., Chen, C. H., Huang, C., Huang, H. Y., Zhang, G. F., Wang, Y. J., Wang, H. L., Lou, S. R., Qiao,
802 L. P., Zhou, M., Chen, M. H., Chen, Y. R., Streets, D. G., Fu, J. S., and Jang, C. J.: Process analysis of
803 regional ozone formation over the Yangtze River Delta, China using the Community Multi-scale Air
804 Quality modeling system, Atmos. Chem. Phys., 12, 10971-10987, https://doi.org/10.5194/acp-12-10971-
805 2012, 2012.
806 Li, W., Liu, X., Zhang, Y., Tan, Q., Feng, M., Song, M., Hui, L., Qu, Y., An, J., and Gao, H.: Insights into
807 the phenomenon of an explosive growth and sharp decline in haze: A case study in Beijing, J. Environ.
808 Sci. (China), 84, 122-132, https://doi.org/10.1016/j.jes.2019.04.015, 2019.
809 Liu, G., Xin, J., Wang, X., Si, R., Ma, Y., Wen, T., Zhao, L., Zhao, D., Wang, Y., and Gao, W.: Impact of
810 the coal banning zone on visibility in the Beijing-Tianjin-Hebei region, Sci. Total Environ., 692, 402-
811 410, https://doi.org/10.1016/j.scitotenv.2019.07.006, 2019a.
812 Liu, H., Wang, X. M., Pang, J. M., and He, K. B.: Feasibility and difficulties of China's new air quality
813 standard compliance: PRD case of PM2.5 and ozone from 2010 to 2025, Atmos. Chem. Phys., 13, 12013-
814 12027, https://doi.org/10.5194/acp-13-12013-2013, 2013a.
815 Liu, Q., Liu, T., Chen, Y., Xu, J., Gao, W., Zhang, H., and Yao, Y.: Effects of aerosols on the surface
816 ozone generation via a study of the interaction of ozone and its precursors during the summer in Shanghai,
817 China, Sci. Total Environ., 675, 235-246, https://doi.org/10.1016/j.scitotenv.2019.04.121, 2019b.
818 Liu, X. G., Li, J., Qu, Y., Han, T., Hou, L., Gu, J., Chen, C., Yang, Y., Liu, X., Yang, T., Zhang, Y., Tian,

https://doi.org/10.5194/acp-2019-966
Preprint. Discussion started: 17 January 2020

H., and Hu, M.: Formation and evolution mechanism of regional haze: a case study in the megacity Beijing, China, Atmos. Chem. Phys., 13, 4501-4514, https://doi.org/10.5194/acp-13-4501-2013, 2013b.

Liu, Z., Hu, B., Ji, D., Cheng, M., Gao, W., Shi, S., Xie, Y., Yang, S., Gao, M., Fu, H., Chen, J., and Wang, Y.: Characteristics of fine particle explosive growth events in Beijing, China: Seasonal variation, chemical evolution pattern and formation mechanism, Sci. Total Environ., 687, 1073-1086, https://doi.org/10.1016/j.scitotenv.2019.06.068, 2019c.

Lu, X., Zhang, L., Chen, Y., Zhou, M., Zheng, B., Li, K., Liu, Y., Lin, J., Fu, T. M., and Zhang, Q.: Exploring 2016–2017 surface ozone pollution over China: source contributions and meteorological influences, Atmos. Chem. Phys., 19, 8339-8361, https://doi.org/10.5194/acp-19-8339-2019, 2019.

Luan, T., Guo, X., Guo, L., and Zhang, T.: Quantifying the relationship between PM2.5 concentration, visibility and planetary boundary layer height for long-lasting haze and fog-haze mixed events in Beijing, Atmos. Chem. Phys., 18, 203-225, https://doi.org/10.5194/acp-18-203-2018, 2018.

Martin, R. V., Jacob, D. J., Yantosca, R. M., Chin, M., and Ginoux, P.: Global and regional decreases in tropospheric oxidants from photochemical effects of aerosols, J. Geophys. Res.: Atmos., 108, https://doi.org/10.1029/2002jd002622, 2003.

Ming, L., Jin, L., Li, J., Fu, P., Yang, W., Liu, D., Zhang, G., Wang, Z., and Li, X.: PM2.5 in the Yangtze River Delta, China: Chemical compositions, seasonal variations, and regional pollution events, Environ. Pollut., 223, 200-212, https://doi.org/10.1016/j.envpol.2017.01.013, 2017.

Muenkel, C., Eresmaa, N., Rasanen, J., and Karppinen, A.: Retrieval of mixing height and dust concentration with lidar ceilometer, Bound-Lay. Meteorol, 124, 117-128, https://doi.org/10.1007/s10546-006-9103-3, 2007.

Ng, N. L., Herndon, S. C., Trimborn, A., Canagaratna, M. R., Croteau, P. L., Onasch, T. B., Sueper, D., Worsnop, D. R., Zhang, Q., Sun, Y. L., and Jayne, J. T.: An Aerosol Chemical Speciation Monitor (ACSM) for Routine Monitoring of the Composition and Mass Concentrations of Ambient Aerosol, Aerosol Sci. Tech., 45, 780-794, https://doi.org/10.1080/02786826.2011.560211, 2011.

Orrling, D., Fitzgerald, E., Ivanov, A., and Molina, M.: Enhanced sulfate formation on ozone-exposed soot, J. Aerosol Sci., 42, 615-620, https://doi.org/10.1016/j.jaerosci.2011.04.004, 2011.

Pathak, R. K., Wu, W. S., and Wang, T.: Summertime PM2.5 ionic species in four major cities of China: nitrate formation in an ammonia-deficient atmosphere, Atmos. Chem. Phys., 9, 1711-1722,

https://doi.org/10.5194/acp-9-1711-2009, 2009.

Pathak, R. K., Wang, T., and Wu, W. S.: Nighttime enhancement of PM2.5 nitrate in ammonia-poor atmospheric conditions in Beijing and Shanghai: Plausible contributions of heterogeneous hydrolysis of N2O5 and HNO3 partitioning, Atmos. Environ., 45, 1183-1191, https://doi.org/10.1016/j.atmosenv.2010.09.003, 2011.

Petzold, A., and Schonlinner, M.: Multi-angle absorption photometry - a new method for the measurement of aerosol light absorption and atmospheric black carbon, J. Aerosol Sci., 35, 421-441, https://doi.org/10.1016/j.jaerosci.2003.09.005, 2004.

Richards, L. W.: COMMENTS ON THE OXIDATION OF NO2 TO NITRATE - DAY AND NIGHT, Atmos. Environ., 17, 397-402, https://doi.org/10.1016/0004-6981(83)90057-4, 1983.

Russell, A. G., Cass, G. R., and Seinfeld, J. H.: ON SOME ASPECTS OF NIGHTTIME ATMOSPHERIC CHEMISTRY, Environ. Sci. Technol., 20, 1167-1172, https://doi.org/10.1021/es00153a013, 1986.

Seinfeld, J. H.: Atmospheric chemistry and physics of air pollution, Wiley, new York, 1986.

Seinfeld, J. H., and Pandis, S. N.: Atmospheric chemistry and physics: from air pollution to climate change, John Wiley & Sons, Inc, 2006.

Sharma, P., Kuniyal, J. C., Chand, K., Guleria, R. P., Dhyani, P. P., and Chauhan, C.: Surface ozone concentration and its behaviour with aerosols in the northwestern Himalaya, India, Atmos. Environ., 71, 44-53, https://doi.org/10.1016/j.atmosenv.2012.12.042, 2013.

Shi, C., Wang, S., Liu, R., Zhou, R., Li, D., Wang, W., Li, Z., Cheng, T., and Zhou, B.: A study of aerosol optical properties during ozone pollution episodes in 2013 over Shanghai, China, Atmos. Res., 153, 235-249, https://doi.org/10.1016/j.atmosres.2014.09.002, 2015.

Sillman, S.: The relation between ozone, NOx and hydrocarbons in urban and polluted rural environments, Atmos. Environ., 33, 1821-1845, https://doi.org/10.1016/s1352-2310(98)00345-8, 1999.

Su, F., Gao, Q., Zhang, Z., Ren, Z., and Yang, X.: Transport Pathways of Pollutants from Outside in Atmosphere Boundary Layer, Res. Environ. Sci., 17, 26-29,40, 2004.

Sun, Y., Zhuang, G., Tang, A., Wang, Y., and An, Z.: Chemical characteristics of PM2.5 and PM10 in haze-fog episodes in Beijing, Environ. Sci. Technol., 40, 3148-3155, https://doi.org/10.1021/es051533g, 2006.

https://doi.org/10.5194/acp-2019-966
Preprint. Discussion started: 17 January 2020

877 Sun, Y., Wang, Z., Dong, H., Yang, T., Li, J., Pan, X., Chen, P., and Jayne, J. T.: Characterization of
878 summer organic and inorganic aerosols in Beijing, China with an Aerosol Chemical Speciation Monitor,
879 Atmos. Environ., 51, 250-259, https://doi.org/10.1016/j.atmosenv.2012.01.013, 2012.
880 Sun, Y. L., Wang, Z. F., Du, W., Zhang, Q., Wang, Q. Q., Fu, P. Q., Pan, X. L., Li, J., Jayne, J., and
881 Worsnop, D. R.: Long-term real-time measurements of aerosol particle composition in Beijing, China:
882 seasonal variations, meteorological effects, and source analysis, Atmos. Chem. Phys., 15, 10149-10165,
883 https://doi.org/10.5194/acp-15-10149-2015, 2015.
884 Tang, G., Zhang, J., Zhu, X., Song, T., Muenkel, C., Hu, B., Schaefer, K., Liu, Z., Zhang, J., Wang, L.,
885 Xin, J., Suppan, P., and Wang, Y.: Mixing layer height and its implications for air pollution over Beijing,
886 China, Atmos. Chem. Phys., 16, 2459-2475, https://doi.org/10.5194/acp-16-2459-2016, 2016.
887 Tie, X., Brasseur, G., Emmons, L., Horowitz, L., and Kinnison, D.: Effects of aerosols on tropospheric
888 oxidants: A global model study, J. Geophys. Res.: Atmos., 106, 22931-22964,
889 https://doi.org/10.1029/2001jd900206, 2001.
890 Tie, X. X., Madronich, S., Walters, S., Edwards, D. P., Ginoux, P., Mahowald, N., Zhang, R. Y., Lou, C.,
891 and Brasseur, G.: Assessment of the global impact of aerosols on tropospheric oxidants, J. Geophys. Res.:
892 Atmos., 110, https://doi.org/10.1029/2004jd005359, 2005.
893 Toh, Y. Y., Lim, S. F., and von Glasow, R.: The influence of meteorological factors and biomass burning
894 on surface ozone concentrations at Tanah Rata, Malaysia, Atmos. Environ., 70, 435-446,
895 https://doi.org/10.1016/j.atmosenv.2013.01.018, 2013.
896 Trainer, M., Parrish, D. D., Goldan, P. D., Roberts, J., and Fehsenfeld, F. C.: Review of observation-
897 based analysis of the regional factors influencing ozone concentrations, Atmos. Environ., 34, 2045-2061,
898 https://doi.org/10.1016/s1352-2310(99)00459-8, 2000.
899 Wang, D., Zhou, B., Fu, Q., Zhao, Q., Zhang, Q., Chen, J., Yang, X., Duan, Y., and Li, J.: Intense
900 secondary aerosol formation due to strong atmospheric photochemical reactions in summer: observations
901 at a rural site in eastern Yangtze River Delta of China, Sci. Total Environ., 571, 1454-1466,
902 https://doi.org/10.1016/j.scitotenv.2016.06.212, 2016.
903 Wang, H., Lu, K., Chen, X., Zhu, Q., Chen, Q., Guo, S., Jiang, M., Li, X., Shang, D., Tan, Z., Wu, Y.,
904 Wu, Z., Zou, Q., Zheng, Y., Zeng, L., Zhu, T., Hu, M., and Zhang, Y.: High N2O5 Concentrations
905 Observed in Urban Beijing: Implications of a Large Nitrate Formation Pathway, Environ. Sci. Tech. Let.,

https://doi.org/10.5194/acp-2019-966
Preprint. Discussion started: 17 January 2020

4, 416-420, https://doi.org/10.1021/acs.estlett.7b00341, 2017a.

Wang, L., Zhang, F., Pilot, E., Yu, J., Nie, C., Holdaway, J., Yang, L., Li, Y., Wang, W., Vardoulakis, S., and Krafft, T.: Taking Action on Air Pollution Control in the Beijing-Tianjin-Hebei (BTH) Region: Progress, Challenges and Opportunities, Int. J. Env. Res. Pub. He., 15, https://doi.org/10.3390/ijerph15020306, 2018.

Wang, L., Liu, J., Gao, Z., Li, Y., Huang, M., Fan, S., Zhang, X., Yang, Y., Miao, S., Zou, H., Sun, Y., Chen, Y., and Yang, T.: Vertical observations of the atmospheric boundary layer structure over Beijing urban area during air pollution episodes, Atmos. Chem. Phys., 19, 6949-6967, https://doi.org/10.5194/acp-19-6949-2019, 2019a.

Wang, T., Xue, L., Brimblecombe, P., Lam, Y. F., Li, L., and Zhang, L.: Ozone pollution in China: A review of concentrations, meteorological influences, chemical precursors, and effects, Sci. Total Environ., 575, 1582-1596, https://doi.org/10.1016/j.scitotenv.2016.10.081, 2017b.

Wang, T., Xue, L. K., Brimblecombe, P., Lam, Y. F., Li, L., and Zhang, L.: Ozone pollution in China: A review of concentrations, meteorological influences, chemical precursors, and effects, Sci. Total Environ., 575, 1582-1596, https://doi.org/10.1016/j.scitotenv.2016.10.081, 2017c.

Wang, W., Li, X., Shao, M., Hu, M., Zeng, L., Wu, Y., and Tan, T.: The impact of aerosols on photolysis frequencies and ozone production in Beijing during the 4-year period 2012–2015, Atmos. Chem. Phys., 19, 9413-9429, https://doi.org/10.5194/acp-19-9413-2019, 2019b.

Wang, X., Zhang, Y., Chen, H., Yang, X., Chen, J., and Geng, F.: Particulate Nitrate Formation in a Highly Polluted Urban Area: A Case Study by Single-Particle Mass Spectrometry in Shanghai, Environ. Sci. Technol., 43, 3061-3066, https://doi.org/10.1021/es8020155, 2009.

Wang, X., Wang, W., Yang, L., Gao, X., Nie, W., Yu, Y., Xu, P., Zhou, Y., and Wang, Z.: The secondary formation of inorganic aerosols in the droplet mode through heterogeneous aqueous reactions under haze conditions, Atmos. Environ., 63, 68-76, https://doi.org/10.1016/j.atmosenv.2012.09.029, 2012.

Wang, Y., Zhuang, G., Zhang, X., Huang, K., Xua, C., Tang, A., Chen, J., and An, Z.: The ion chemistry, seasonal cycle, and sources of PM2.5 and TSP aerosol in Shanghai, Atmos. Environ., 40, 2935-2952, https://doi.org/10.1016/j.atmosenv.2005.12.051, 2006.

Wang, Y., Zhang, Q. Q., He, K., Zhang, Q., and Chai, L.: Sulfate-nitrate-ammonium aerosols over China: response to 2000-2015 emission changes of sulfur dioxide, nitrogen oxides, and ammonia, Atmos. Chem.

https://doi.org/10.5194/acp-2019-966
Preprint. Discussion started: 17 January 2020

Phys., 13, 2635-2652, https://doi.org/10.5194/acp-13-2635-2013, 2013.

Wang, Z., Pan, X., Uno, I., Li, J., Wang, Z., Chen, X., Fu, P., Yang, T., Kobayashi, H., Shimizu, A., Sugimoto, N., and Yamamoto, S.: Significant impacts of heterogeneous reactions on the chemical composition and mixing state of dust particles: A case study during dust events over northern China, Atmos. Environ., 159, 83-91, https://doi.org/10.1016/j.atmosenv.2017.03.044, 2017d.

Wen, L., Xue, L. K., Wang, X. F., Xu, C. H., Chen, T. S., Yang, L. X., Wang, T., Zhang, Q. Z., and Wang, W. X.: Summertime fine particulate nitrate pollution in the North China Plain: increasing trends, formation mechanisms and implications for control policy, Atmos. Chem. Phys., 18, 11261-11275, https://doi.org/10.5194/acp-18-11261-2018, 2018.

Yao, X. H., Chan, C. K., Fang, M., Cadle, S., Chan, T., Mulawa, P., He, K. B., and Ye, B. M.: The water-soluble ionic composition of PM2.5 in Shanghai and Beijing, China, Atmos. Environ., 36, 4223-4234, https://doi.org/10.1016/s1352-2310(02)00342-4, 2002.

Zeng, P., Lyu, X. P., Guo, H., Cheng, H. R., Jiang, F., Pan, W. Z., Wang, Z. W., Liang, S. W., and Hu, Y. Q.: Causes of ozone pollution in summer in Wuhan, Central China, Environ. Pollut., 241, 852-861, https://doi.org/10.1016/j.envpol.2018.05.042, 2018.

Zhao, D., Xin, J., Gong, C., Quan, J., Liu, G., Zhao, W., Wang, Y., Liu, Z., and Song, T.: The formation mechanism of air pollution episodes in Beijing city: Insights into the measured feedback between aerosol radiative forcing and the atmospheric boundary layer stability, Sci. Total Environ., 692, 371-381, https://doi.org/10.1016/j.scitotenv.2019.07.255, 2019.

Zhong, J., Zhang, X., Wang, Y., Sun, J., Zhang, Y., Wang, J., Tan, K., Shen, X., Che, H., Zhang, L., Zhang, Z., Qi, X., Zhao, H., Ren, S., and Li, Y.: Relative Contributions of Boundary-Layer Meteorological Factors to the Explosive Growth of PM2.5 during the Red-Alert Heavy Pollution Episodes in Beijing in December 2016, J. Meteorol. Res., 31, 809-819, https://doi.org/10.1007/s13351-017-7088-0, 2017.

Zhong, J., Zhang, X., Dong, Y., Wang, Y., Liu, C., Wang, J., Zhang, Y., and Che, H.: Feedback effects of boundary-layer meteorological factors on cumulative explosive growth of PM2.5 during winter heavy pollution episodes in Beijing from 2013 to 2016, Atmos. Chem. Phys., 18, 247-258, https://doi.org/10.5194/acp-18-247-2018, 2018.

Zhu, X., Tang, G., Lv, F., Hu, B., Cheng, M., Muenkel, C., Schafer, K., Xin, J., An, X., Wang, G., Li, X., and Wang, Y.: The spatial representativeness of mixing layer height observations in the North China Plain,

https://doi.org/10.5194/acp-2019-966
Preprint. Discussion started: 17 January 2020

Atmospheric Chemistry and Physics Discussions

964 Atmos. Res., 209, 204-211, https://doi.org/10.1016/j.atmosres.2018.03.019, 2018.